Dear Dr Schymanski and anonymous reviewers,

Thank you for the opportunity to revise our manuscript, and for your helpful and insightful comments. We have submitted a revised version, which has taken into account all of the comments and we hope presents a more robust piece of work.

As has already been communicated to the editor, in the course of addressing Reviewer 2's points about whether it was reasonable to carry out the attribution analysis at the regional and annual scale and why the fitted and attributed trends in E_PA were so different, we discovered that there was indeed a bug in the code that calculated the attribution. We thank you for your patience while we addressed the revised results. The bug had the effect of artificially suppressing the contribution of the temperature, humidity and wind speed to the rate of change of PET. This was responsible for the marked difference between the attributed and the fitted trend, particularly for the aerodynamic component. Now that the bug has been fixed, the trends are consistent between the linear regression and the sum-of-components. We have edited the table of percentage contributions as suggested by reviewer 2, to be percentages of the fitted trend to illustrate this.

The dominant contribution to the positive PET trend now comes from the air temperature, but this is largely cancelled out by the trend in humidity and windspeed. The radiation components are still relatively large, and the downward shortwave still has a large effect on the spring PET, so we have retained the discussion of aerosol and circulation effects.

We have submitted a revised manuscript, and a version with changes highlighted, as requested. We implemented the changes as described in our responses to the reviewers, and as requested by the editor. We address specific points from the editor's comments below. All other changes are as defined in our previous responses to the reviewers. Finally, this document also contains the marked-up version of the paper showing the changes. Note that line numbers below refer to the new submitted paper, not the marked-up version.

Regards,

Emma Robinson, on behalf of the authors.

Response to editor

1. We have added objectives at the end of the introduction, and return to them in the conclusion. We have also included discussion of other regional studies of PET and its trends and attribution in the introduction.

2. In Section 2.10 we have included some discussion of data validation that we have carried out with meteorological data from UK flux sites, which are independent of the synoptic stations from which the MORECS data are derived. Unfortunately these observations are not long enough to calculate robust trends (the longest is 10 years), but we have looked at the comparison of daily and monthly means with the appropriate squares from the gridded data and provided statistics to show the good agreement between the gridded data and the observations. We have also pointed the reader to discussions of uncertainty in the original data papers where appropriate.

   Note that none of the flux sites have pan evaporation data sets available, so this suggestion could not be implemented.

3. We have retained the Penman-Monteith formulation, and retained the ‘interception corrected’ PETI as well. PM potential evaporation with an interception component is known and used by hydrologists, so we do still wish to discuss what difference it makes. We have improved our description of the interception component in Section 3.1 and hope that it makes it clear that the PETI assumes that a wet canopy has a potential evaporation with no stomatal/canopy resistance, a dry canopy has potential evaporation with stomatal resistance = 70 sm-1, and an intermediate canopy has potential evaporation which is a linear combination of the two, dependent on how wet the canopy is.

   We have further discussed the choice of using Penman-Monteith PET defined for a reference crop in Section 3, and we continue to use this rather than the Penman formulation because of its inclusion of the effect of vegetation.

   While we do agree that investigating the PM equation with different resistances would be interesting, it is outside of the scope of this paper.

   We have taken the advice to use the phrase “atmospheric evaporative demand” (or AED) throughout the text.

4. Due to the suggestion from Reviewer 2 we have recalculated the attribution by calculating the results for each pixel, then calculated a weighted mean over each region. We have also continued with the analysis on the regional means, as this allows us to calculate more conservative confidence intervals (otherwise it is difficult to account for spatial correlation in the trend maps). We also discuss the product-of-means vs mean-of-products issue, and note that our seasonal and annual analyses ultimately give the same results.

5. We have included both a table of absolute values of the contributions, and a table of the contributions as a percentage of the linear regression to PET (and the radiative and aerodynamic components).

6. We agree that the description of Fig 11 (now Fig 13) was not adequate, but we also decided that the figure itself could be improved. We have rearranged the figure, and rewritten the legend, and hope that this serves to clarify the results.

   As mentioned above, in investigating the results, we realised that there was indeed a problem with the numerics (the code was artificially supressing the contributions of air temperature, humidity and wind speed relative to the contributions of the LW and SW radiation). We have fixed this and the results are more consistent with other regional and global studies.

7. We have presented trend maps in the appendix as requested.

8. The original test we carried out of constant vs varying air pressure in the specific humidity calculation was for the whole of the dataset, not just the uplands, and it makes only a few percent difference in all regions. Apologies that this was not clear before. We have included

some discussion of this in the text.

9. We have more clearly identified where CRU, WFD, GEAR and MORECS data were used.

10. We have added some of these points to the text.

11. The DTR is included in the meteorological data set as it is required for some models (particularly the JULES LSM), so we have clarified why we have included it, despite it not being used for the PET calculations.

    Because MORECS only provides daily mean air temperature, the DTR was obtained from the CRU TS 3.21 data. We have clarified this in the text (see point 9).

12. We have added relative differences to the PET maps (Fig. 6) and climatology plots (Fig. 7).

Other changes

1. We have added a section about validation of the meteorological data (Section 2.10). This includes references for some variables, and description of validation carried out against meteorological observations from four UK flux sites.

2. We have added some more detail about interception inhibiting transpiration to the manuscript (lines 362-376), to make it clear that it is not simply that the intercepted water is directly blocking the stomata.

3. We have investigated the reviewer's suggestions about product-of-mean vs mean-of-products. This gives the same results to within a few percent, but have mentioned this in the manuscript (lines 538-548)

   As mentioned above, we found a bug in the code, and now recover the fitted trends more successfully.

4. Table 3: We now give the contributions as percentages of the actual trend (although it is now Table 4, not table 3).

5. Trend maps: We have included trend maps in Appendix B

6. We have kept the constant 100kPa air pressure in the calculation of specific humidity, but have mentioned that this makes only a small difference (lines 182-184)

   We have included some discussion of the vapour pressure lapse rate and have changed the citation (lines 167-168)

7. We have discussed the choice of vapour pressure lapse rate for adjusting the humidity for height (lines 170-175)

8. Line 149-152. We have clarified which variables come from data sources other than MORECS

9. Line 225-226. We have added a note that if the method does not allow negative wind speed

10. Line 237-239. We have explained why we have not interpolated DTR

11. Line 246-248: We have more clearly explained the adjustment of air pressure with elevation.

12. Fig 1. We have improved the choice of limits on the colour maps

13. Figs 6, 7. We have added relative difference to the PET maps and climatology plots.

14. Line 239-240. We have clarified the role of DTR in this dataset.

15. Trends per year vs. trends per decade: We have made these consistent through the text

16. Line 466-471: The evidence for drying summers is over a much longer time period than this dataset, we have clarified this in the text.

17. Figure 13 caption: We have altered the plot and the caption.

18. Eqs 2, 9, 10: We have corrected typos

19. q has been changed to q_a where necessary throughout

20. A typo in Equation 4 has been fixed.

21. Line 352: Wind speed was added to the list

22. P has been changed to PET where necessary

23. Line 297-305: We have added more discussion of the particular choice of PET in this paper.

24. Line 334-347: We have added to the discussion of a constant standard reference surface.

25. Introduction: We have expanded the discussion of regional studies within a global context, and of previous studies looking at trends in PET and reference crop evaporation

26. Line 47: We changed 'physical drivers' to 'climate drivers', as this study does not include the effects of land use change etc.

27. We have added objectives to the introduction and added a conclusion section

28. Line 138-139: We have added more detail about the variables.

29. Line 186-187: Hours of bright sunshine definition has been included.

30. We will change rainfall to precipitation throughout.

31. Line 156-157: We have quantified where islands have been excluded.

32. Line 230: Reference to natural neighbour interpolation will be added.

33. Line 439: We have added references to Oldekop and Andréassian.

34. Line: 513-515: Added a discussion of Matsoukas results being based on reanalysis output

35. Table 1: Added reference height for radiation

36. Added letter labels to plots where necessary

37. Line 390-295: Added a discussion of snow

38. Line 450-452: Changed the sentence about allowing for non-zero lag-1 autocorrelation

39. Added 95% CIs on trends throughout

40. Line 614-615: Added trends for SW down

Trends in atmospheric evaporative demand in Great Britain using high-resolution meteorological data

Emma L. Robinson[1], Eleanor M. Blyth[1], Douglas B. Clark[1], Jon Finch[1] and Alison C. Rudd[1]

[1]{Centre for Ecology and Hydrology, Maclean Building, Benson Lane, Crowmarsh Gifford, Wallingford OX10 8BB}

Correspondence to: Emma L. Robinson (emrobi@ceh.ac.uk)

Abstract

Observations of climate are often available on very different spatial scales from observations of the natural environments and resources that are affected by climate change. In order to help bridge the gap between these scales using modelling, a new dataset of daily meteorological variables was created at 1 km resolution over Great Britain for the years 1961-2012, by interpolating coarser resolution climate data and including the effect of local topography. These variables were used to calculate atmospheric evaporative demand (AED) at the same spatial and temporal resolution~~, both excluding~~. Two functions that represent AED were chosen: one is a standard form of Potential Evapotranspiration (PET) and ~~including (PETI)~~the other is a derivative of it used by hydrologists that includes the effect of water intercepted by the canopy~~.~~ (PETI). Temporal trends in ~~evaporative demand~~these functions were calculated, with PET found to ~~increase at a rate of~~ be increasing in all regions~~ and~~, and at an overall rate of 0.021±0.021 mm d^{-1} decade^{-1} in Great Britain, while PETI was found to ~~increase~~be increasing at a rate 0.023±0.023 mm d^{-1} decade^{-1} in England~~.~~ (0.028±0.025 mm d^{-1} decade^{-1} in the English Lowlands), but not increasing at a statistically significant rate in Scotland or Wales. The trends ~~and~~ were found to vary by season, with spring ~~evaporative demand~~PET increasing by ~~14% (11%~~0.043±0.019 mm d^{-1} decade^{-1} (0.038±0.018 mm d^{-1} decade^{-1} when the interception correction is included) in Great Britain~~ over the dataset~~, while there is no statistically significant trend in other seasons. The trends ~~in PET~~ were attributed analytically to trends in the climate variables~~, with~~; the ~~spring~~overall positive trend ~~in evaporative demand being~~was predominantly driven by rising air temperature, although rising specific humidity had a negative effect on the trend. Increasing downward short- and longwave radiation ~~trends,~~made an overall positive contribution to the PET trend, while the 10 m wind speed had a negative effect. The trend in spring PET was particularly ~~by increasing solar~~strong due to a strong increase in spring downward shortwave radiation.

1 Introduction

~~There are many studies showing the ways in which our living environment is changing over time: wildlife surveys in the UK of both flora (Wood et al., 2015; Evans et al., 2008) and fauna (Pocock et al., 2015) show a shift in patterns and timing~~ There are many studies showing the ways in which our living environment is changing over time: changing global temperatures (IPCC, 2013), radiation (Wild, 2009) and wind speeds ~~(Thackeray et al., 2010)~~(McVicar et al., 2012)~~. In addition, the UK natural resources of freshwater (Watts et al., 2015), soils (Reynolds et al., 2013; Bellamy et al., 2005) and vegetation~~ can have significant impacts on ecosystems and human life (IPCC, 2014a). While there are overall global trends, the impacts can vary between regions (IPCC, 2014b). In the UK, wildlife surveys of both flora ~~(Berry et al., 2002; Hickling et al., 2006; Norton et al., 2012)~~(Wood et al., 2015; Evans et al., 2008)~~ are changing. We are experiencing new environmental stresses on the land and water systems of the UK through changes in temperature and rainfall (Crooks and Kay, 2015; Watts et al., 2015; Hannaford, 2015).~~

~~To explain these changes in terms of physical drivers, there are several gridded meteorological datasets available for Great Britain. Some are derived directly from observations – for example the Met Office Rainfall and Evaporation Calculation System (MORECS) dataset~~ and fauna (Pocock et al., 2015) show a shift in patterns and timing ~~(Thompson et al., 1981; Hough and Jones, 1997)~~(Thackeray et al., 2010)~~, the UKCP09 observed climate data (Jenkins et al., 2008) and the Climate Research Unit time series 3.21 (CRU TS 3.21) data~~. In addition, the UK natural resources of freshwater (Watts et al., 2015), soils ~~(Unit et al., 2013; Harris et al., 2014)~~(Reynolds et al., 2013; Bellamy et al., 2005)~~ – while some use global meteorological reanalyses bias-corrected to observations – for example the WATCH Forcing Data (WFD;~~ and vegetation ~~Weedon et al. (2011)~~(Berry et al., 2002; Hickling et al., 2006; Norton et al., 2012)~~) and WATCH Forcing Data methodology applied to ERA-Interim reanalysis product (WFDEI; Weedon et al. (2014)) and the Princeton Global Meteorological Forcing Dataset (Sheffield et al., 2006).~~

~~However, while observations of carbon, methane and water emissions from the land (Baldocchi et al., 1996), the vegetation cover (Morton et al., 2011) and soil properties (FAO/IIASA/ISRIC/ISS-CAS/JRC, 2012) are typically made at the finer landscape scale of 100 m to 1000 m, most long-term meteorological datasets are only available at a relatively coarse resolution of a few tens of km. These spatial scales may not be representative of the~~

~~climate experienced by the flora and fauna being studied, and it has also been shown that input resolution can have a strong effect on the performance of hydrological models (Kay et al., 2015). In addition, the coarse temporal resolution of some datasets, for example the monthly CRU TS 3.21 data (Harris et al., 2014; Unit et al., 2013), can miss important sub-monthly extremes. It is imperative for our increased understanding and improved analysis of the environment that we bridge the gap between the scales of observations with modelling. However, while there are datasets available at higher spatial and temporal resolutions (such as UKCP09 (Jenkins et al., 2008)), these often do not provide all the variables needed for land surface or hydrological modelling.~~

~~To address this, we have created a meteorological dataset for Great Britain at the landscape scale: 1 km (Robinson et al., 2015a).~~ are changing. The UK is experiencing new environmental stresses on the land and water systems through changes in temperature and river flows (Crooks and Kay, 2015; Watts et al., 2015; Hannaford, 2015), which is part of a widespread global pattern of temperature increase and circulation changes (Watts et al., 2015).

To explain these changes in terms of climate drivers, there are several gridded meteorological datasets available at global and regional scales. Global datasets can be based on observations – for example the 0.5° resolution Climate Research Unit time series 3.21 (CRU TS 3.21) data (Jones and Harris, 2013; Harris et al., 2014) – while some are based on global meteorological reanalyses bias-corrected to observations – for example the WATCH Forcing Data (WFD, 0.5°; Weedon et al. (2011)), the WATCH Forcing Data methodology applied to ERA-Interim reanalysis product (WFDEI, 0.5°; Weedon et al. (2014)) and the Princeton Global Meteorological Forcing Dataset (1°; Sheffield et al. (2006)). At the regional scale in Great Britain (GB), there are datasets that are derived directly from observations – for example the Met Office Rainfall and Evaporation Calculation System (MORECS) dataset at 40 km resolution (Thompson et al., 1981; Hough and Jones, 1997) and the UKCP09 observed climate data at 5 km resolution (Jenkins et al., 2008).

However, while regional observations of carbon, methane and water emissions from the land (Baldocchi et al., 1996), the vegetation cover (Morton et al., 2011) and soil properties (FAO/IIASA/ISRIC/ISS-CAS/JRC, 2012) are typically made at the finer landscape scale of 100 m to 1000 m, most of these long-term gridded meteorological datasets are only available at a relatively coarse resolution of a few tens of km. These spatial scales may not be representative of the climate experienced by the flora and fauna being studied, and it has also been shown that input resolution can have a strong effect on the performance of hydrological models (Kay et al., 2015). In addition, the coarse temporal resolution of some datasets, for example the monthly CRU TS 3.21 data (Harris et al., 2014; Jones and Harris, 2013), can miss important sub-monthly extremes.

Regional studies are important to identify drivers and impacts of changing meteorology that may or may not be reflected in trends in global means. For example, in Canada (Vincent et al., 2015) and Europe (Fleig et al., 2015), high resolution meteorological data have been used to identify the impacts of changing circulation patterns, while in Australia wind speed data have been used to quantify the effects of global stilling in the region (McVicar et al., 2008). While there are datasets available at finer spatial and temporal resolutions for the UK (such as UKCP09 (Jenkins et al., 2008)), these often do not provide all the variables needed to identify the impacts of changing climate.

To address this, we have created a meteorological dataset for Great Britain at 1 km resolution (Robinson et al., 2015a). It is derived from the observation-based MORECS dataset ~~(Thompson et al., 1981; Hough and Jones, 1997)~~(Thompson et al., 1981; Hough and Jones, 1997), ~~which is~~and then downscaled using information about topography. This is augmented by an independent precipitation dataset – Gridded Estimates of daily and monthly Areal Rainfall for the United Kingdom (CEH-GEAR; ~~Tanguy et al. (2014); Keller et al. (2015)~~Tanguy et al. (2014); Keller et al. (2015)) – along with variables from two global datasets – WFD ~~Weedon et al. (2011)~~ and CRU TS 3.21 ~~(Harris et al., 2014; Unit et al., 2013)~~ – to produce a comprehensive, observation-based, daily meteorological dataset at 1 km × 1 km spatial resolution.

~~In addition, a key variable in hydrological modelling is the evaporative demand of the atmosphere, which is determined by the meteorological variables (Kay et al., 2013). Hydrological models such as Climate and Land use Scenario Simulation in Catchments (CLASSIC; Crooks and Naden (2007)) and Grid-to-Grid (G2G; Bell et al. (2009)) and metrics such as the Palmer Drought Severity Index (PDSI; Palmer (1965)) require potential evapotranspiration – an estimate of the unstressed evaporative demand of the atmosphere – as an input. While hydrological models can make use of high resolution topographic information and precipitation datasets, they are often driven with potential evapotranspiration calculated at a coarser resolution (Bell et al., 2011; Bell et al., 2012; Kay et al., 2015). Therefore, we have also created a potential evapotranspiration dataset, consisting of two estimates of potential~~

~~evapotranspiration, which can be used to run high-resolution hydrological models (Robinson et al., 2015b).~~

~~This paper presents the method of creation of the new high-resolution meteorological and potential evaporation datasets. Regional trends in evaporative demand are then calculated and attributed to regional trends in the meteorological data.~~

In order to understand the effect of meteorology on the water cycle, a key variable in hydrological modelling is the atmospheric evaporative demand (AED), which is determined by meteorological variables (Kay et al., 2013). It has been shown that water-resource and hydrological model results are largely driven by how this property is defined and used (Haddeland et al., 2011). The AED can be expressed in several ways, for instance the evaporation from a wet surface, from a well-watered but dry uniform vegetated cover, or from a hypothetical well-watered but dry version of the actual vegetation. Metrics such as the Palmer Drought Severity Index (PDSI; Palmer (1965)) use potential evapotranspiration (PET) as an input while many hydrological models such as Climate and Land use Scenario Simulation in Catchments (CLASSIC; Crooks and Naden (2007)) or Grid-to-Grid (G2G; Bell et al. (2009)), use as input a distinct form of the PET which includes the intercepted water from rainfall (this is described later in the text) which we hereby name PETI. While hydrological models can make use of high resolution topographic information and precipitation datasets, they are often driven with PET calculated at a coarser resolution (Bell et al., 2011; Bell et al., 2012; Kay et al., 2015). Therefore, we have also created a dataset consisting of estimates of PET and PETI, which can be used to run high-resolution hydrological models (Robinson et al., 2015b).

Other regional studies have created gridded estimates of AED in Austria (Haslinger and Bartsch, 2016) and Australia (Donohue et al., 2010). Regional studies of trends in AED have seen varied results, with increasing AED seen in Romania (Paltineanu et al., 2012), Serbia (Gocic and Trajkovic, 2013), Spain (Vicente-Serrano et al., 2014), some regions of China (Li and Zhou, 2014) and Iran (Azizzadeh and Javan, 2015; Hosseinzadeh Talaee et al., 2013; Tabari et al., 2012), decreasing AED in north east India (Jhajharia et al., 2012) and regions in China (Yin et al., 2009; Song, 2010; Shan et al., 2015; Zhao et al., 2015; Zhang et al., 2015; Lu et al., 2016) and regional variability in Australia (Donohue et al., 2010) and China (Li et al., 2015). In order to understand this variability, it is important to quantify the relative contributions of the changing meteorological variables to trends in AED and regional studies often find different drivers of changing AED (see McVicar et al. (2012) for a review). Relative humidity has been shown to drive AED in the Canary Islands (Vicente-Serrano et al., 2016), wind speed and air temperature were shown to have nearly equal but opposite effects in Australia (Donohue et al., 2010), while in China sunshine hours (Li et al., 2015), wind speed (Yin et al., 2009) or a combination of the two (Lu et al., 2016) have been shown to drive trends. Rudd and Kay (2015) investigated projected changes in PET using a regional climate model, but little has been done to investigate historical trends of AED in the UK.

The objectives of this paper are (i) to evaluate the trends in key meteorological variables in Great Britain over the years 1961-2012; (ii) to evaluate the AED in Great Britain over the same time period; (iii) to investigate the effect of including interception in the formulation of PET called PETI; (iv) to evaluate trends in PET over the time period of interest; and (v) to attribute the trends in PET to trends in meteorological variables. To address these objectives, the paper is structured as follows. Section 2 presents the calculation of the meteorological variables. Section 3 presents the calculation of PET and PETI from the meteorological variables and assesses the difference between PET and PETI. In Section 4 the trends in annual means of the meteorological variables and AED are calculated and the trends in PET are attributed to trends in meteorological variables. In Section 5 the results are discussed and conclusions are presented in Section 6.

2 Calculation of meteorological variables

The meteorological variables included in this new dataset ~~(Robinson et al., 2015a) are~~(Robinson et al., 2015a) are daily mean values of air temperature, specific humidity, wind speed, downward ~~long~~ longwave (LW) and shortwave (SW) radiation, precipitation~~,~~ and air pressure, plus daily temperature range ~~and air pressure~~ (Table 1). These variables are important drivers of near-surface conditions, and, for instance, are the full set of variables required to drive the JULES land surface model (LSM) ~~(Best et al., 2011; Clark et al., 2011)~~(Best et al., 2011; Clark et al., 2011)~~.~~, as well as other LSMs.

The data were derived primarily from MORECS, which is a long-term gridded dataset starting in 1961 and updated to the present ~~(Thompson et al., 1981; Hough and Jones, 1997)~~(Thompson et al., 1981; Hough and Jones, 1997). It interpolates five ~~daily synoptic station~~ variables ~~(~~from synoptic stations (daily mean values of air temperature, vapour pressure~~,~~ and wind speed, daily hours of bright sunshine~~, rainfall~~ and daily total precipitation) to a 40 km × 40 km resolution grid aligned with the Ordnance Survey National Grid. There are currently 270 stations reporting in real time, while a further 170 report the daily readings on a monthly basis, but numbers have varied throughout the run. The algorithm interpolates a varying number of stations (up to nine) for each square, depending on data availability (Hough and Jones, 1997). The interpolation is such that the value in each grid square is the effective measurement of a station positioned at the centre of the square and at the grid square mean elevation, averaged from ~~09~~00:00 GMT to ~~09~~00:00 GMT the next day. MORECS is a consistent, quality-controlled time series, which accounts for changing station coverage. The MORECS variables were used to derive the air temperature, specific humidity, wind speed, downward ~~long-~~LW and ~~shortwave~~SW radiation and air pressure in the new dataset. The WFD and CRU TS 3.21 datasets were used ~~where variables~~for surface air pressure and daily temperature range respectively, as they could not be calculated ~~solely~~ from MORECS~~, except for~~. Additionally precipitation~~, for which~~ was obtained from the CEH-GEAR data~~ were used instead of interpolating the MORECS rainfall. ~~, which is a product directly interpolated to 1 km from the station data (Keller et al., 2015).

The spatial coverage of the dataset was determined by the spatial coverage of MORECS, which covers the majority of Great Britain, but excludes some coastal regions and islands at the 1 km scale. For ~~many~~most of these points, the interpolation was extended from the nearest MORECS squares, but some outlying islands (in particular Shetland and the Scilly Isles) were ~~deemed to be too far~~excluded when the entire island was further than 40 km from ~~any~~the nearest MORECS ~~squares and were therefore excluded~~square.

2.1 Air temperature

Air temperature, T_a (K), was derived from the MORECS air temperature. The MORECS air temperature was reduced to mean sea level, using a lapse rate of -0.006 K m^{-1} ~~(Hough and Jones, 1997).~~(Hough and Jones, 1997). A bicubic spline was used to interpolate from 40 km resolution to 1 km resolution, then the temperatures were adjusted to the elevation of each 1 km square using the same lapse rate. The 1 km resolution elevation data used were aggregated from the Integrated Hydrological Digital Terrain Model (IHDTM) – a 50 m resolution digital terrain model ~~(Morris and Flavin, 1990)~~(Morris and Flavin, 1990).

2.2 Specific humidity

Specific humidity, q_a (kg kg^{-1}), was derived from the MORECS vapour pressure, which was first reduced to mean sea level, using a lapse rate of -0.025 % m^{-1} ~~(Hough and Jones, 1997).~~ (Thompson et al., 1981). The actual lapse rate of humidity will, in general, vary according to atmospheric conditions. However, calculating this would require more detailed information than is available in the input data used. Any method of calculating the variation of specific humidity with height will involve several assumptions, but the method used here is well-established and is used by the Met Office in calculating MORECS (Thompson et al., 1981). The value of the vapour pressure lapse rate is chosen to keep relative humidity constant with altitude, rather than assuming that the specific humidity itself is constant.

A bicubic spline was used to interpolate vapour pressure to 1 km resolution then the ~~vapour pressure~~ values were adjusted to the 1 km resolution elevation using the IHDTM elevations ~~(Sect. 2.1).~~. Finally the specific humidity was calculated, ~~assuming a constant air pressure, p_* = 100000 Pa,~~ using

$$q_a = \frac{\epsilon e}{p_* - (1-\epsilon)e}, \quad (1)$$

~~where e is the vapour pressure (Pa) and ϵ = 0.622 is the mass ratio of water to dry air (Gill, 1982).~~

where e is the vapour pressure (Pa) and ϵ = 0.622 is the mass ratio of water to dry air (Gill, 1982). The air pressure, p_*, in this calculation was assumed to have a constant value of 100000 Pa because this was prescribed in the computer code. It would be better to use a varying air pressure, as calculated in Section 2.8, but this makes a negligible difference (of a few percent) to the calculated specific humidity and a constant p_* was retained.

2.3 Downward shortwave radiation

~~Downward shortwave radiation, S_d (W m^{-2}), was derived from the MORECS hours of bright sunshine. The sunshine hours were used to calculate the cloud cover factor, $C_f = n/N$, where n is the number of hours of bright sunshine in a day, and N is the total number of hours between sunrise and sunset. The cloud cover factor was interpolated to 1 km resolution using a bicubic spline. The downward shortwave solar radiation for a horizontal plane at the Earth's surface was calculated using the solar angle equations of Iqbal (1983) and a form of the Angstrom-Prescott equation which relates hours of bright sunshine to solar irradiance (Ångström, 1918; Prescott, 1940), with empirical coefficients calculated by Cowley (1978). The Cowley coefficients vary spatially and seasonally and effectively account for reduction of irradiance with increasing solar zenith angle, as well as implicitly accounting for spatially- and seasonally-~~

varying aerosol effects. However, they do not vary interannually and thus do not explicitly include long-term trends in aerosol concentration.

In addition, the downward shortwave radiation was corrected for the average inclination and aspect of the surface, assuming that only the direct beam radiation is a function of the inclination and that the diffuse radiation is homogeneous. It was also assumed that the cloud cover is the dominant factor in determining the diffuse fraction (Muneer and Munawwar, 2006). The aspect and inclination were calculated using the IHDTM elevation at 50 m resolution, following the method of Horn (1981), and were then aggregated to 1 km resolution. The top of atmosphere flux for horizontal and inclined surfaces was calculated following Allen et al. (2006) and the ratio used to scale the direct beam radiation.

Downward SW radiation, S_d (W m^{-2}), was derived from the MORECS hours of bright sunshine (defined as the total number of hours in a day for which solar irradiation exceeds 120 W m^{-2} (WMO, 2013)). The value calculated is the mean SW radiation over 24 hours. The sunshine hours were used to calculate the cloud cover factor, $C_f = n/N$, where n is the number of hours of bright sunshine in a day, and N is the total number of hours between sunrise and sunset (Marthews et al., 2011). The cloud cover factor was interpolated to 1 km resolution using a bicubic spline. The downward SW solar radiation for a horizontal plane at the Earth's surface was then calculated using the solar angle equations of Iqbal (1983) and a form of the Angstrom-Prescott equation which relates hours of bright sunshine to solar irradiance (Ångström, 1918; Prescott, 1940), with empirical coefficients calculated by Cowley (1978). They vary spatially and seasonally and effectively account for reduction of irradiance with increasing solar zenith angle, as well as implicitly accounting for spatially- and seasonally-varying aerosol effects. However, they do not vary interannually and thus do not explicitly include long-term trends in aerosol concentration.

The downward SW radiation was then corrected for the average inclination and aspect of the surface, assuming that only the direct beam radiation is a function of the inclination and that the diffuse radiation is homogeneous. It was also assumed that the cloud cover is the dominant factor in determining the diffuse fraction (Muneer and Munawwar, 2006). The aspect and inclination were calculated using the IHDTM elevation at 50 m resolution, following the method of Horn (1981), and were then aggregated to 1 km resolution. The top of atmosphere flux for horizontal and inclined surfaces was calculated following Allen et al. (2006) and the ratio used to scale the direct beam radiation.

2.4 Downward longwave radiation

Downward ~~longwave~~LW radiation, L_d (W m^{-2}), was derived from the 1 km resolution air temperature (Sect. 2.1), vapour pressure (Sect. 2.2) and cloud cover factor (Sect. 2.3~~). The downward longwave radiation for clear sky conditions was calculated as a function of air temperature and precipitable water using the method of Dilley and O'Brien (1998), with precipitable water calculated from air temperature and humidity following Prata (1996). The additional component due to cloud cover was calculated using the equations of Kimball et al. (1982), assuming a constant cloud base height of 1000 m.~~

). The downward LW radiation for clear sky conditions was calculated as a function of air temperature and precipitable water using the method of Dilley and O'Brien (1998), with precipitable water calculated from air temperature and humidity following Prata (1996). The additional component due to cloud cover was calculated using the equations of Kimball et al. (1982), assuming a constant cloud base height of 1000 m.

2.5 Wind speed

The ~~10 m~~ wind speed at a height of 10 m, u_{10} (m s^{-1}), was derived from the MORECS 10 m wind speed~~. The MORECS wind speed data~~, which were interpolated to 1 km resolution using a bicubic spline and adjusted for topography using a 1 km resolution dataset of mean wind speeds produced by the UK Energy Technology Support Unit (ETSU) ~~(Newton and Burch, 1985; Burch and Ravenscroft, 1992).~~(Newton and Burch, 1985; Burch and Ravenscroft, 1992). This used Numerical Objective Analysis Boundary Layer (NOABL) methodology and station wind measurements over the period 1975-84 to produce a map of mean wind speed over the UK. To calculate the topographic correction, the ETSU wind speed was aggregated to 40 km resolution, then the difference between each 1 km value and the corresponding 40 km mean found. This difference was added to the interpolated daily wind speed. In cases where this would result in a negative wind speed, the wind speed was set to zero.

2.6 Precipitation

Precipitation rate, P (kg m^{-2} s^{-1}), is taken from the daily CEH-GEAR dataset ~~(Tanguy et al., 2014; Keller et al., 2015)~~(Tanguy et al., 2014; Keller et al., 2015), scaled to the appropriate units. The CEH-GEAR methodology uses natural neighbour interpolation ~~to interpolate synoptic station data to a 1 km resolution gridded daily precipitation dataset of the estimated~~

~~rainfall~~(Gold, 1989) to interpolate synoptic station data to a 1 km resolution gridded daily dataset of the estimated precipitation in 24 hours between 09:00 GMT and 09:00 GMT the next day.

2.7 Daily temperature range

Daily temperature range (DTR), D_T (K), was obtained from the CRU TS 3.21 monthly mean daily temperature range estimates on a 0.5° latitude × 0.5° longitude grid, which is interpolated from monthly climate observations ~~(Harris et al., 2014; Unit et al., 2013)~~(Harris et al., 2014; Jones and Harris, 2013)~~. These~~. There is no standard way to correct DTR for elevation, so these data were reprojected to the 1 km grid with no interpolation and the monthly mean used to populate the daily values in each month. Although DTR is not required in the calculation of AED, it is a required input of the JULES LSM, in order to run at sub-daily timestep.

2.8 Surface air pressure

Surface air pressure, p_* (Pa), was derived from the WFD, an observation-corrected reanalysis product, which provides 3 hourly meteorological data for 1958-2001 on a 0.5° latitude × 0.5° longitude resolution grid ~~(Weedon et al., 2011)~~(Weedon et al., 2011). Mean monthly values of WFD surface air pressure and air temperature were calculated for each 0.5° grid box over the years 1961-2001. These were reprojected to the 1 km grid with no interpolation, then the ~~air temperature used to lapse the air pressure from the WFD elevation to the 1 km resolution elevation using the temperature lapse rate specified in Sect. 2.1 (Shuttleworth, 2012).~~lapse rate of air temperature (Sect. 2.1) used to calculate the integral of the hypsometric equation, in order to obtain the air pressure at the elevation of each 1 km grid (Shuttleworth, 2012). The mean monthly values were used to populate the daily values in the full dataset, thus the surface air pressure in the new dataset does not vary interanually~~.~~, but does vary seasonally. This is reasonable as the trend in surface air pressure in the WFD is negligible~~.~~ (Weedon et al., 2011).

2.9 Spatial and seasonal patterns of meteorological variables

Long-term mean values of ~~each~~the meteorological ~~variable~~variables were calculated for each 1 km square over the whole dataset (1961-2012) (Fig. 1). Four~~Mean monthly climatologies (Fig. 2) were calculated over the whole of Great Britain (GB), and over four~~ sub-regions of interest were defined (Fig. ~~3). Three~~2); three of these regions correspond to ~~the~~ nations (England, Wales and Scotland), while the fourth is the 'English lowlands', a subset of ~~the English region, which includes~~England, covering south-central and south-east England, East Anglia and the East Midlands (Folland et al., 2015). Mean-monthly climatologies (Fig. ~~(Folland et al., 2015).~~ 3) were calculated over the whole of Great Britain (GB), and over these four regions of interest.

The maps clearly show the effect of topography on the variables (Fig. 1), with an inverse correlation between elevation and temperature, specific humidity, downward ~~longwave~~LW radiation and surface air pressure and a positive correlation with wind speed. The precipitation has an east-west gradient due to prevailing weather systems and orography. The fine-scale structure of the downward ~~shortwave~~SW radiation is due to the aspect and elevation of each grid cell, with more spatial variability in areas with more varying terrain. As no topographic correction has been applied to DTR, it varies only on a larger spatial scale. Although specific humidity is inversely proportional to elevation, relative humidity is not, as the saturated specific humidity will also be inversely proportional to elevation due to the decrease in temperature with height.

The mean-monthly climatologies (Fig. ~~2~~3) demonstrate the differences between the regions, with Scotland generally ~~being cooler~~having lower temperatures and ~~wetter~~more precipitation than the average, and England (particularly the English lowlands) being warmer and drier.

2.10 Validation of meteorology

The precipitation dataset, CEH-GEAR, has previously been validated against observations (Keller et al., 2015). Other studies discuss the uncertainties in the CRU TS 3.21 daily temperature range data (Harris et al., 2014) and WFDEI air pressure data (Weedon et al., 2014).

For the other variables, the MORECS data set is ultimately derived from the synoptic stations around the UK which represent most of the available observed meteorological data. The only way to validate the gridded meteorology presented here is to compare it to independently observed data, which are available at a few sites where meteorological measurement stations are located. Here we carry out a validation exercise with data from four sites from the UK, which have meteorological measurements available for between 5 and 10 years. Details of the sites and data are in Appendix A. Fig. 4 shows the comparison of data set air temperature with the observed air temperature at each of the four sites. This shows a strong correlation (r^2 between 0.94 and 0.97) between the data set and the observations. Fig. 5 shows the mean-monthly climatology calculated from both the data set and from the observations (only for times for which observations were available) and demonstrates that the data set successfully captures the seasonal cycle. This has been repeated for downward SW radiation and for an estimate of the mixing ratio of water vapour, 10 m wind speed and surface air pressure (Appendix A). The air temperature, downward SW radiation and mixing ratio all have high correlations and represent the seasonal cycle well. The wind speed is overestimated by the derived data set at two sites, which is likely to be due to land cover effects. The modelling which produced the ETSU dataset uses topography but not land cover (Burch and Ravenscroft, 1992; Newton and Burch, 1985), so at sites with tall vegetation the wind speed is likely to be less than the modelled value. The air pressure has a low correlation because the data set contains a mean-monthly climatological value. However, the mean bias is low and the RMSE is small, confirming that it is reasonable to use a climatological value in place of daily data.

3 Calculation of potential evapotranspiration (PET)

~~The Penman-Monteith potential evapotranspiration (PET), E_P (mm dy^{-1}), is a physically-based formulation of the evaporative demand of the atmosphere (Monteith, 1965). It is calculated from the daily meteorological variables using the equation~~

~~$$E_p = \frac{t_d}{\lambda}\frac{\Delta A + \frac{c_p \rho_a}{r_a}(q_s - q_a)}{\Delta + \gamma\left(1 - \frac{r_s}{r_a}\right)}, \qquad (2)$$~~

There are several ways to assess the evaporative demand of the atmosphere. Pan evaporation can be modelled using the Pen-Pan model, or open-water evaporation can be modelled with the Penman equation. However, neither of these account for the fact that in general the evaporation is occurring from a vegetated surface. A widely used model is the Penman-Monteith PET, E_P (mm d^{-1}, equivalent to kg m^{-2} d^{-1}), which is a physically-based formulation of the AED of the atmosphere (Monteith, 1965). It provides an estimate of AED dependent on the atmospheric conditions but allowing for the fact that that the water is evaporating through the surface of leaves and thus the resistance is higher. It is calculated from the daily meteorological variables using the equation

$$E_P = \frac{t_d}{\lambda}\frac{\Delta A + \frac{c_p \rho_a}{r_a}(q_s - q_a)}{\Delta + \gamma\left(1 + \frac{r_s}{r_a}\right)}, \qquad (2)$$

where t_d = 86400 s d^{-1} is the length of a day ~~in seconds~~, λ=2.5×10^{6} J kg^{-1} is the latent heat of evaporation, q_s is saturated specific humidity (kg kg^{-1}), Δ is the gradient of saturated specific humidity with respect to temperature (kg kg^{-1} K^{-1}), A is the available energy (W m^{-2}), c_p=1010

J kg^{-1} K^{-1} is the specific heat capacity of air, ρ_a is the density of air (kg m^{-3}), ~~q~~q_a is specific humidity (kg kg^{-1}), γ=0.004 K^{-1} is the psychrometric constant, r_s is stomatal resistance (s m^{-1}) and r_a is aerodynamic resistance (s m^{-1}~~).~~) (Stewart, 1989).

The saturated specific humidity, q_s (kg kg^{-1}), is calculated from saturated vapour pressure, e_s (Pa), using Eq. (1). The saturated vapour pressure is calculated using an empirical fit to air temperature

$$e_s = p_s exp\left(\sum_{i=1}^{4} a_i \left(1-\frac{T_s}{T_a}\right)^i\right)\qquad (3)$$

where p_s = 101325 Pa is the steam point pressure, T_s = 373.15 K is the steam point temperature and a=(13.3185, -1.9760, -0.6445, -0.1299) are empirical coefficients ~~(Richards, 1971).~~(Richards, 1971).

The derivative of the saturated specific humidity with respect to temperature, Δ (kg kg^{-1} K^{-1}), is therefore

$$\Delta = \frac{T_s}{T_a^2}\frac{p_* q_s}{p_*-(1-\epsilon)e_s}\sum_{i=1}^{4} i a_i \left(1-\frac{T_s}{T_a}\right)^{i-1}\qquad (4)$$

The available energy, A (W m^{-2}), is the energy balance of the surface,

$$A = R_n - G\qquad (5)$$

where R_n is the net radiation (W m^{-2}) and G is the soil heat flux (W m^{-2}). The net soil heat flux is negligible at the daily timescale ~~(Allen et al., 1998)~~(Allen et al., 1998), so the available energy is equal to the net radiation, such that

$$A = (1-\alpha)S_d + \varepsilon(L_d - \sigma T_*^4)\qquad (6)$$

~~where σ is the Stefan-Boltzmann constant, α is the albedo and ε the emissivity of the surface and T_* is the surface temperature (Shuttleworth, 2012). For this study the surface temperature is approximated by using the air temperature, T_a. The albedo and emissivity are also dependent on the land cover; for a well-watered grass surface an albedo of 0.23 and an emissivity of 0.92 are used (Allen et al., 1998).~~

~~The air density, ρ_a (kg m^{-3}), is a function of air pressure and temperature,~~

$\rho_a = \frac{p_*}{rT_a}$, where σ is the Stefan-Boltzmann constant, α is the albedo and ε the emissivity of the surface and T_* is the surface temperature (Shuttleworth, 2012). For this study the surface temperature is approximated by using the air temperature, T_a.

The air density, ρ_a (kg m^{-3}), is a function of air pressure and temperature,

$$\rho_a = \frac{p_*}{rT_a}, \quad (7)$$

where r = 287.05 J kg^{-1} K^{-1} is the gas constant of air.

The stomatal and aerodynamic resistances are strongly dependent on the land cover due to differences in roughness length and physiological constraints on transpiration of different vegetation types. Following Allen et al. (1998) the PET was calculated for an FAO-defined standard well-watered grass surface, which has stomatal resistance r_s = 70.0 s m^{-1}.

Again following Allen et al. (1998), aerodynamic resistance, r_a (s m^{-1}), is a function of the 10 m wind speed

$r_a = \frac{278}{u_{10}}$. The stomatal and aerodynamic resistances are strongly dependent on land cover due to differences in roughness length and physiological constraints on transpiration of different vegetation types. In addition, the albedo and emissivity are also dependent on the land cover. In order to investigate the effect of meteorology on AED, as distinct from land use effects, the PET was calculated for a single land cover type over the whole of the domain. If necessary, this can be adjusted to give an estimate of PET specific to the local land cover, for example using regression relationships (Crooks and Naden, 2007). As a standard, the Food and Agriculture Organization of the United Nations (FAO) calculate reference crop evaporation for a hypothetical reference crop, which corresponds to a well-watered grass (Allen et al., 1998). Following this, the PET in the current study was calculated for a reference crop of 0.12 m height, with constant stomatal resistance, r_s = 70.0 s m^{-1}, an albedo of 0.23 and emissivity of 0.92 over the whole of Great Britain. This study therefore neglects the effect of land-use on evaporation, which could be investigated in future by calculating PET for different land surface types, with different coverage for each year of the dataset.

Following Allen et al. (1998), the aerodynamic resistance, r_a (s m^{-1}), is a function of the 10 m wind speed

$$r_a = \frac{278}{u_{10}}. \quad (8)$$

Thus the PET is a function of six of the meteorological variables: air temperature, specific humidity, downward long LW and shortwaveSW radiation, wind speed and surface air pressure.

The PET can be split between two factors, the radiative component, E_{PR},

To explore the role of the different meteorological variables in the AED, it is helpful to split the radiative component (the first part of the numerator in Equation 2) from the wind component (the second part). Formally, this is defined as follows (Doorenbos, 1977):

The radiative component, E_{PR},

$$E_{PR} = \frac{t_d}{\lambda} \frac{\Delta A}{\Delta+\gamma\left(1-\frac{r_s}{r_a}\right)}, \frac{\Delta A}{\Delta+\gamma\left(1+\frac{r_s}{r_a}\right)},$$

(9)

and the aerodynamic component, E_{PA},

$$E_{PA} = \frac{t_d}{\lambda} \frac{\frac{c_p \rho_a}{r_a}(q_s-q_a)}{\Delta+\gamma\left(1-\frac{r_s}{r_a}\right)}, \frac{\frac{c_p \rho_a}{r_a}(q_s-q_a)}{\Delta+\gamma\left(1+\frac{r_s}{r_a}\right)},$$

(10)

such that $E_P = E_{PR} + E_{PA}$.

3.1 Potential evapotranspiration pluswith interception (PETI)

When rain falls, water is intercepted by the canopy. The evaporation of this intercepted water is not constrained by stomatal resistance but is subject to the same aerodynamic resistance, defined by the roughness of the canopy, as transpiration, but is not constrained by stomatal resistance (Shuttleworth, 2012) (Shuttleworth, 2012). At the same time, leaves covered with water cannot transpire, so interception inhibits transpiration from the wet fraction of the canopy (Ward and Robinson, 2000). transpiration is inhibited in a wet canopy. Suppression of transpiration is well observed both by comparing eddy-covariance fluxes and observations of sap flow (Kume et al., 2006; Moors, 2012), and by observing stomatal and photosynthesis response to wetting (Ishibashi and Terashima, 1995). For plants which have at least some of their stomata on the upper surface of the leaves, this can be due to water directly blocking the stomata. However, in GB most plants have stomata only on the underside of the leaves, so the transpiration is inhibited by other mechanisms.

Physically, the suppression may simply be due to the fact that energy is used in evaporating the intercepted water, so less is available for transpiration (Bosveld and Bouten, 2003) or that the increased humidity of the air, due to evaporation of intercepted water, causes the stomata to close (Lange et al., 1971). It may also be due to the presence of water causing stomatal closure through physiological reactions, which can be observed even when the stomata are on the underside of a leaf and the water is lying on the upper side (Ishibashi and Terashima, 1995).

In the short term after a rain event, potential water losses due to evaporation may be underestimated if only potential transpiration is calculated~~.~~, and therefore overall rates underestimated. As transpiration is inhibited over the wet fraction of the canopy (Ward and Robinson, 2000) , the PET over a grid box will be a linear combination of the potential interception and potential transpiration, each weighted by the fraction of the canopy that is wet or dry. This can be accounted for by introducing an interception term to the calculation of ~~potential evaporation. If the daily rainfall is greater than zero, then the rain is used to fill (part of) the canopy and this store evaporates~~PET, giving PETI. This is modelled as an interception~~,~~ store, which is (partially) filled by rainfall, proportionally inhibiting the transpiration. ~~On~~As the interception store dries, the relative contribution of interception is decreased and the transpiration increases. This correction is applied on days with precipitation, while on days without ~~rain~~precipitation, the potential ~~evaporation~~ is equal to the ~~potential transpiration~~ PET defined in Eq. 2. ~~A~~Although an unconventional definition of PET, a similar interception correction is applied to the ~~potential evapotranspiration~~PET provided at 40 km resolution by MORECS ~~(Thompson et al., 1981).~~(Thompson et al., 1981) which is used widely by hydrologists.

~~The potential evapotranspiration plus interception (PETI) is a function~~This method implicitly assumes that the water is liquid, however snow lying on the canopy will also inhibit transpiration, and will be depleted by melting as well as by sublimation. The rates may be slower, and the snow may stay on the canopy for longer than one day. However, the difference of accounting for canopy snow as distinct from canopy water will have a small effect on large-scale averages, as the number of lying snow days in GB is relatively low, and they occur during winter when the PET is very small.

The PETI is a weighted sum of the PET, E_P, (as calculated ~~above)~~in Eq 2.) and potential interception, E_I, which is calculated by substituting zero stomatal resistance, r_s=0 s m^{-1}, into Eq. ~~(~~2~~)~~.. To calculate the relative proportions of interception and transpiration, it is assumed that the wet fraction of the canopy is proportional to the amount of water in the interception store ~~and that transpiration is only possible through the fraction of the canopy which is dry.~~. The interception store, S_I (kg m^{-2}), decreases through the day according to an exponential dry down ~~(Rutter et al., 1971)~~(Rutter et al., 1971), such that

$$S_I(t) = S_o e^{-\frac{E_I}{S_{tot}}t}, e^{-\frac{E_I}{S_{tot}}t}. \qquad (11)$$

where E_I is the potential interception, S_{tot} is the total capacity of the interception store (kg m^{-2}), S_0 is the precipitation that is intercepted by the canopy (kg m^{-2}) and t is the time (in days) since a rain event. The total capacity of the interception store is calculated following ~~Best et al. (2011),~~Best et al. (2011), such that

$$S_{tot} = 0.5 + 0.05\Lambda, \Lambda. \qquad (12)$$

~~where Λ is the leaf area index (LAI); for the FAO standard grass land cover the LAI is 2.88 (Allen et al., 1998). The fraction of rainfall intercepted by the canopy is found also following Best et al. (2011), assuming that rainfall lasts for an average of 3 hours.~~

where Λ is the leaf area index (LAI); for the FAO standard grass land cover the LAI is 2.88 (Allen et al., 1998). The fraction of precipitation intercepted by the canopy is found also following Best et al. (2011), assuming that precipitation lasts for an average of 3 hours.

The wet fraction of the canopy, C_{wet}, is proportional to the store size, such that

$$C_{wet}(t) = \frac{S(t)}{S_{tot}}; . \qquad (13)$$

The total PETI is the sum of the interception from the wet canopy and the transpiration from the dry canopy,

$$E_{PI}(t) = E_I C_{wet}(t) + E_P\left(1 - C_{wet}(t)\right); . \qquad (14)$$

This is integrated over one day to find the total PETI, E_{PI} (mm ~~dy~~d^{-1}), to be

$$E_{PI} = S_0\left(1 - e^{-\frac{E_I}{S_{tot}}}\right) + E_P\left(1 - \frac{S_0}{E_I}\left(1 - e^{-\frac{E_I}{S_{tot}}}\right)\right); . \qquad (15)$$

The PETI is a function of the same six meteorological variables as the PET, plus the precipitation.

3.2 Spatial and seasonal patterns of ~~potential evaporation~~PET and PETI

Both PET and PETI have a distinct gradient from low in the north-west to high in the south-east, and they are both inversely proportional to the elevation (Fig. ~~4~~6), reflecting the spatial patterns of the meteorological variables. The PETI is 8 % higher than the PET overall but this difference is larger in the north and west, where precipitation rates, and therefore interception, are higher (Fig. ~~4~~6). In Scotland, the higher interception and lower ~~evaporative demand~~AED mean that this increase is a larger proportion of the total, with the mean PETI being ~~10~~11 % larger than the PET (in some areas the difference is more than 25%). In the English lowlands the difference is ~~more moderate~~smaller, at 6 %, but ~~it~~this is a more water limited region where hydrological modelling can be sensitive to even relatively small adjustments to ~~potential evaporation~~PET (Kay et al., 2013).

The seasonal climatology of both PET and PETI follow the meteorology (Fig. ~~5~~7), with high values in the summer and low in the winter. ~~The~~Although the relative difference peaks in winter, the absolute difference between PET and PETI is bimodal, with a peak in March and a smaller peak in October (September in Scotland) (Fig. ~~5~~7), because in winter the overall ~~evaporative demand~~AED is low, while in summer the amount of ~~rainfall~~precipitation is low, so the interception correction is small. The seasonal cycle of PET is driven predominantly by the radiative component, which has a much stronger seasonality than the aerodynamic component (Fig. ~~6~~8).

On a monthly or annual timescale, the ratio of PET to precipitation is an indicator of the wet- or dryness of a region ~~(Kay et al., 2013).~~(Oldekop, 1911; Andréassian et al., 2016). Low values of PET relative to precipitation indicate wet regions, where evaporation is demand-limited, while high values indicate dry, water-limited regions. In the wetter regions (Scotland, Wales) mean-monthly PET and PETI (Fig. ~~5~~7) are on average lower than the mean-monthly precipitation (Fig. ~~2~~3) throughout the year, while in drier regions (England, English lowlands) the mean PET and PETI are higher than the precipitation for much of the summer, highlighting the ~~region's~~regions' susceptibility to hydrological drought (Folland et al., 2015).

4 Decadal trends

4.1 Meteorological Variables

Annual means of the meteorological variables (Fig. ~~7~~9) and the PET and PETI (Fig. ~~8~~10) were calculated for each ~~of the five regions.~~region. The trends in these annual means were calculated using linear regression; the significance (*P* value) and 95% confidence intervals (CI) of the slope are calculated ~~assuming a~~specifically allowing for the non-zero lag-1 autocorrelation, to account for possible ~~correlation~~correlations between adjacent data points ~~(von Storch and Zwiers, 1999; Zwiers and von Storch, 1995)~~(Zwiers and von Storch, 1995; von Storch and Zwiers, 1999). In addition, seasonal means were calculated, with the four seasons defined to be Winter (December-February~~,~~), Spring (March-May~~,~~), Summer (June-August) and Autumn (September-November~~,~~), and trends in these means were also found.

The trends ~~and associated 95% confidence intervals of the annual means for Great Britain of the meteorological variables~~ can be seen in Table 2. ~~The trends in the annual and seasonal means for all regions are plotted in Fig. 9; trends that are statistically significant at the 5% level are plotted with solid error bars, those that are not significant are plotted with dashed lines. There was a statistically significant trend in air temperature in all regions (except in winter), which agrees with recent trends in the Hadley Centre Central England Temperature (HadCET) dataset (Parker and Horton, 2005) and in temperature records for Scotland (Jenkins et al., 2008) as well as in the CRUTEM4 dataset (Jones et al., 2012). An increase in winter precipitation in Scotland is seen in the current dataset, but no significant trends otherwise. Long term observations show that there has been little trend in annual precipitation, but a change in seasonality with wetting winters and drying summers (Jenkins et al., 2008). The statistically significant decline in wind speed in all regions is consistent with the results of McVicar et al. (2012) and Vautard et al. (2010), who report decreasing wind speeds in the northern hemisphere over the late 20th century.~~

The trends in the annual and seasonal means for all regions are plotted in Fig. ~~The slopes and associated 95 % confidence intervals of PET and PETI for annual means over Great Britain~~11; trends that are statistically significant at the 5% level are plotted with solid error bars, those that are not significant are plotted with dashed lines. The analysis was repeated for each pixel in the 1 km resolution dataset; maps of these rates of change can be seen in Appendix B.

There was a statistically significant trend in air temperature in all regions (except in winter), which agrees with recent trends in the Hadley Centre Central England Temperature (HadCET) dataset (Parker and Horton, 2005) and in temperature records for Scotland (Jenkins et al., 2008) as well as in the CRUTEM4 dataset (Jones et al., 2012). An increase in winter precipitation in Scotland is seen in the current dataset, which leads to a statistically significant increase in the annual mean precipitation of GB. However, all other regions and seasons have no statistically significant trends in precipitation. Long term observations show that there has been little trend in annual precipitation, but a change in seasonality with wetting winters and drying summers since records began, although with little change over the past 50 years (Jenkins et al., 2008). The statistically significant decline in wind speed in all regions is consistent with the results of McVicar et al. (2012) and Vautard et al. (2010), who report decreasing wind speeds in the northern hemisphere over the late 20th century.

4.2 Potential Evapotranspiration

The trends of the meteorological variables are interesting in their own right. But for hydrology, it is the impact that the trends have on evaporation that matters and that depends on their combination, which can be expressed through PET.

The regional trends of annual mean PET and PETI can be seen in Table 2, and the trends in the annual and seasonal means of PET, PETI, and the radiative and aerodynamic components of PET are plotted in Fig. ~~10~~12 for all regions. Maps of the trends can be seen in Appendix B. The trend in the radiative component of PET is positive over the whole of GB. However, the trend in the aerodynamic component varies; for much of Wales, Scotland and northern England, it is not significant, or is slightly negative, while in south-east England and north-west Scotland it is positive. This leads to a positive trend in PET over much of GB, but no significant trend in southern Scotland and northern England. There is a statistically significant increase in annual PET in all regions except Wales; the GB trend (0.021±0.021 mm ~~dy~~d^{-1} decade^{-1}) is equivalent to an increase of 0.11±0.11 mm ~~dy~~d^{-1} (8.3±8.1 % of the long term mean) over the whole dataset. Increases in PETI are only statistically significant in England (0.023±0.023 mm ~~dy~~d^{-1} decade^{-1}) and English lowlands (0.028±0.025 mm ~~dy~~d^{-1} decade^{-1}), where the increases over the whole dataset are 0.12±0.12 mm ~~dy~~d^{-1} (8.0±8.0 % of the long term mean) and 0.15±0.13 mm ~~dy~~d^{-1} (~~10~~9.7±8.8 % of the long term mean) respectively. There is a difference in trend between different seasons. In winter, summer and autumn there are no statistically significant trends in PET or PETI, other than the English lowlands in autumn, but the spring is markedly different, with very significant trends (P<0.0005) in all regions. The GB spring trends in PET (0.043±0.019 mm ~~dy~~d^{-1} decade^{-1}) and PETI (0.038±0.018 mm ~~dy~~d^{-1} decade^{-1}) are equivalent to an increase of 0.22±0.10 mm ~~dy~~d^{-1} (~~14~~13.8±6.2 % of the long-term spring mean) and 0.20±0.09 mm ~~dy~~d^{-1} (11.2±5.3 % of the long-term spring mean) over the length of the dataset respectively. The radiative component of PET has similarly significant trends in spring, while the aerodynamic component has no significant trends in any season (Fig. ~~10~~12), indicating that the trend in PET is due to the increasing radiative component.

There are few studies of long-term trends in ~~evaporative demand~~AED in the UK. MORECS provides an estimate of Penman-Monteith PET with interception correction calculated directly from the 40 km resolution meteorological data ~~(Hough and Jones, 1997; Thompson et al., 1981)~~(Hough and Jones, 1997; Thompson et al., 1981), and increases can be seen over the dataset ~~(Rodda and Marsh, 2011).~~(Rodda and Marsh, 2011). But as the PET and PETI in the current dataset are ultimately calculated using the same meteorological data (albeit by different methods), it is not unexpected that similar trends should be seen. Site-based studies suggest an increase over recent decades ~~(Burt and Shahgedanova, 1998; Crane and Hudson, 1997)~~(Burt and Shahgedanova, 1998; Crane and Hudson, 1997), but it is difficult to separate climate-driven trends from local land-use trends. ~~The~~A global review paper ~~by (McVicar et al., 2012)~~(McVicar et al., 2012) ~~identifies a trend of decreasing evaporative demand in the northern hemisphere, driven by decreasing wind speeds, however they also report significant local variations on trends in pan evaporation, including the increasing trend observed by Stanhill and Möller (2008) at a site in England after 1968. Matsoukas et al. (2011) identify a statistically significant increase in potential evaporation in several regions of the globe, including southern England, between 1983 and 2008, attributing it predominantly to an increase in the radiative component of PET, due to global brightening.~~

identified a trend of decreasing AED in the northern hemisphere, driven by decreasing wind speeds, however they also reported significant local variations on trends in pan evaporation, including the increasing trend observed by Stanhill and Möller (2008) at a site in England after 1968. Matsoukas et al. (2011) identified a statistically significant increase in PET in several regions of the globe, including southern England, between 1983 and 2008, attributing it predominantly to an increase in the radiative component of PET, due to global brightening. However, these results were obtained using reanalysis data, which is limited in its ability to capture trends in wind speed. This limitation has been documented in both northern (Pryor et al., 2009) and southern (McVicar et al., 2008) hemispheres.

Regional changes in actual evaporative losses can be estimated indirectly using regional precipitation and runoff or river flow. Using a combination of observations and modelling, ~~Marsh and Dixon (2012) identified an increase in evaporative losses in Great Britain from 1961-2011. Hannaford and Buys (2012)~~Marsh and Dixon (2012) identified an increase in evaporative losses in Great Britain from 1961-2011. Hannaford and Buys (2012) note seasonal and regional differences in trends in observed river flow, suggesting that decreasing spring flows in the English lowlands are indicative of increasing ~~evaporative demand.~~AED. However, changing evaporative losses can also be due to changing supply through precipitation, so it is important to formally attribute the trends in ~~potential evaporation~~PET to changing climate, in order to understand changing ~~evaporative losses~~evapotranspiration.

~~4.1~~4.3 Attribution of trends in potential evapotranspiration

In order to attribute changes in PET to changes in climate, the rate of change of PET, $\mathrm{d}E_p/\mathrm{d}t$~~,~~ ~~can be calculated as a function of the rate of change of each variable (Donohue et al., 2010)~~ (mm d^{-1} decade^{-1}), can be calculated as a function of the rate of change of each variable (Roderick et al., 2007),

$$\frac{\mathrm{d}E_P}{\mathrm{d}t} = \frac{\mathrm{d}E_P}{\mathrm{d}T_a}\frac{\mathrm{d}T_a}{\mathrm{d}t} + \frac{\mathrm{d}E_P}{\mathrm{d}q_a}\frac{\mathrm{d}q_a}{\mathrm{d}t} + \frac{\mathrm{d}E_P}{\mathrm{d}u_{10}}\frac{\mathrm{d}u_{10}}{\mathrm{d}t} + \frac{\mathrm{d}E_P}{\mathrm{d}L_d}\frac{\mathrm{d}L_d}{\mathrm{d}t} + \frac{\mathrm{d}E_P}{\mathrm{d}S_d}\frac{\mathrm{d}S_d}{\mathrm{d}t} \quad (16)$$

Note that we exclude the surface air pressure, because this dataset uses a mean-monthly climatology as the interannual variability of air pressure is negligible. The derivative of the PET with respect to each of the meteorological variables can be found analytically (Appendix ~~A~~C). The derivatives are calculated from the daily meteorological data~~, then the overall annual and regional means found.~~ at 1 km resolution. Substituting the slopes of the linear regressions of the gridded annual means (Appendix B~~Fig. 9~~) for the rate of change of each variable with time, and the overall time-average of the derivatives of PET with respect to the meteorological variables, the contribution of each variable to the rate of change of PET can be calculated~~.~~ at 1 km resolution. These are then averaged over the regions of interest. The same can also be applied to the radiative and aerodynamic components independently.

~~Figure 11~~Note that this can also be applied to the regional means of the derivatives of PET and the trends in the meteorological variables. The results are compared in Table 3 and the two approaches are consistent. For the regional analysis, we also quote the 95% CI. However, for the gridded values, there is such high spatial coherence that combining the 95% CI over the region results in unreasonably constrained results. We therefore use the more conservative CI obtained from the regional analysis. Also note that this method assumes that the rate of change of the variables with respect to time is constant over the whole dataset (and thus the product of the means is equal to the mean of the products), and indeed this is how it is often applied (Donohue et al., 2010; Lu et al., 2016). The effect of this assumption was investigated by repeating the analysis with seasonal trends and means, but this makes negligible difference to the results.

Fig. 13 shows the contribution of each meteorological variable to the rate of change of the annual mean PET and to the radiative and aerodynamic components~~.~~ and compares the total attributed trend to that obtained by linear regression. The percentage contribution is ~~seen in Table 3. The radiative component has no dependence on specific humidity, while~~in Table 4, calculated as a fraction of the fitted trend. The final columns shows the total attributed trend as a percentage of the fitted trend, to demonstrate the success of the attribution at recovering the fitted trends. For the PET trend and for the trend in the radiative component, these values generally sum to the linear regression to within a few percent. However, for the aerodynamic component~~ has no dependence on long- or shortwave radiation.~~

~~The rate of change of PET is almost entirely due to the change in the~~ , the fitted trend is very small (an order of magnitude smaller than the PET and radiative component~~. In all regions except Scotland, the change in the radiative component of PET is dominated by the increase due to the increasing downward shortwave radiation, followed by the increasing downward longwave radiation, while in Scotland the effect of the downward shortwave is smaller. In all regions there is also a small increase in the radiative component due to the decreasing wind speed, and a decrease due to increasing air temperature, but these are negligible compared to the effect of changing radiation. Increasing air temperature contributes to a small increase in the aerodynamic component of PET, but this is offset by the decrease due to increasing specific humidity and decreasing wind speed, so that overall the change in the aerodynamic component~~ trends), and much smaller than the statistical uncertainty. This means that there can be a large and/or negative percentage difference between the attributed and fitted trends, even when the absolute difference is negligible.

The largest overall contribution to the rate of change of PET comes from increasing air temperature, which has the effect of increasing the aerodynamic component (as it makes the air more able to hold water), but it decreases the radiative component (due to increasing outgoing LW radiation). However, the decrease due to increasing specific humidity largely cancels this increase in the aerodynamic component. Overall the next largest increases are caused by increasing downward SW radiation, particularly in the English regions in the spring, as it increases the radiative component of PET. However, in Scotland and Wales, the increasing downward LW radiation is also important. Finally, the decreasing wind speed has the effect of increasing the radiative component, but decreasing the aerodynamic component, so overall it tends to cause a decrease in PET.

Since the increasing air temperature and downward LW and SW radiation have the effect of increasing PET, but the increasing specific humidity and decreasing wind speed tend to decrease it, then the overall trend is positive, but smaller than the trend due to air temperature alone.

5 Discussion

These high resolution datasets provide ~~an~~ insight into the effect of the changing climate of Great Britain on ~~evaporative demand~~AED over the past five decades. There have been significant climatic trends in the UK since 1961; in particular rising air temperature and specific humidity, decreasing wind speed and decreasing cloudiness. ~~The resulting trends in downward long- and shortwave radiation have combined to lead to trends in evaporative demand.~~Although some are positive and some negative, these meteorological trends combine to give statistically significant trends in PET.

Wind speeds have decreased more significantly in the west than the east, and show a consistent decrease across seasons. Contrary to ~~Donohue et al. (2010)~~Donohue et al. (2010) and ~~McVicar et al. (2012),~~McVicar et al. (2012), this study finds that the change in wind speed of the late 20th and early 21st centuries has had a negligible influence on PET over the period of study. However, the previous studies were concerned with open-water Penman evaporation, which has a simpler (proportional) dependence on wind speed than the Penman-Monteith ~~potential evaporation~~PET considered here~~. Although the significant decrease in wind speed has had a negligible effect on evaporative demand, it may nonetheless have had a direct effect on biodiversity (Barton, 2014; Brittain et al., 2013) and implications for wind energy resources (Sinden, 2007)~~(Schymanski and Or, 2015).

The air temperature trendstrend in this study of around 0.221±0.15 K decade^{-1} arein GB is consistent with observed global and regional trends (Hartmann et al., 2013; Jenkins et al., 2008)(Hartmann et al., 2013; Jenkins et al., 2008). The temperature trend also does not explicitly make a large contribution to the trend in PET, but is partly responsible for the trend of increasing downward longwave radiation. The trends in longwave radiation in these datasets are not statistically significant, due to high inter-annual variability, but contribute to between 22% and 50% of the trends in PET and the radiative component (Table 3). Observations of longwave radiation are often uncertain, but, although small, the trend in this dataset is consistent with observed trends (Wang and Liang, 2009), as well as with trends in the WFDEI bias-corrected reanalysis product (Weedon et al., 2014).

. The temperature trend is responsible for a large contribution to the trend in PET, although the large negative contribution from the specific humidity (as well as a small negative contribution from wind speed) means that the overall trend is smaller than the temperature trend alone.

Although the contribution is smaller than that of air temperature, the trends in LW radiation in these datasets contribute to between 15% and 28% of the trends in PET and between 27% and 46% or the trends in the radiative component. Observations of LW radiation are often uncertain, but the trend in this dataset, although small, is consistent with observed trends (Wang and Liang, 2009), as well as with trends in the WFDEI bias-corrected reanalysis product (Weedon et al., 2014).

Increasing solar radiation has been shown to have a strong effect onincrease spring and annual evaporative demandAED, contributing to between 4618% and 7750% of the fitted trend in annual PET (Table 3), increasing , and to between 8443% and 8753% of the fitted trend in spring PET. Two main mechanisms can be responsible for changing solar radiation – changing cloud cover and changing aerosol concentrations. Changing aerosol emissions have been shown to have had a significant effect on solar radiation in the 20th century. In Europe, global dimming due to increased aerosol concentrations peaked around 1980, followed by global brightening as aerosol concentrations decreased (Wild, 2009).(Wild, 2009). Observations of changing continental runoff and river flow in Europe over the 20th century have been attributed to changing aerosol concentrations, via their effect on solar radiation, and thus evaporative demand (Gedney et al., 2014)AED (Gedney et al., 2014).

In this study we use the duration of bright sunshine to calculate the solar radiation, using empirical coefficients which do not vary with year, so aerosol effects are not explicitly included.

The coefficients used in this study to convert sunshine hours to radiation fluxes were empirically derived in 1978; the derivation used data from the decade 1966-75, as this period was identified to be before reductions in aerosol emissions had begun to significantly ~~increase~~alter observed solar radiation ~~(Cowley, 1978).~~(Cowley, 1978). Despite this, the trend in ~~shortwave~~SW radiation in the current dataset from 1979 onwards (1.4±1.4 W m^{-2} decade^{-1}) is consistent, within uncertainties, with that seen over GB in the WFDEI data~~,~~ (0.9±1.1 W m^{-2} decade^{-1}), which is bias-corrected to observations and includes explicit aerosol effects (Weedon et al., 2014).

It has been suggested that aerosol effects also implicitly affect sunshine duration ~~(Helmes and Jaenicke, 1986).~~since in polluted areas, there will be fewer hours above the official 'sunshine hours' threshold of 120 Wm^{-2} (Helmes and Jaenicke, 1986). Several regional studies have shown trends in sunshine hours that are consistent with the periods of dimming and brightening across the globe ~~(eg Liley, 2009; Sanchez-Lorenzo et al., 2009; Sanchez-Lorenzo et al., 2008; Stanhill and Cohen, 2005)~~(eg Liley, 2009; Sanchez-Lorenzo et al., 2009; Sanchez-Lorenzo et al., 2008; Stanhill and Cohen, 2005), and several have attempted to quantify the relative contribution of trends in cloud cover and aerosol loading (e.g. ~~Sanchez-Lorenzo and Wild (2012)~~Sanchez-Lorenzo and Wild (2012) in Switzerland, see ~~Sanchez-Romero et al. (2014)~~Sanchez-Romero et al. (2014) for a review). Therefore, it may be that some of the brightening trend seen in the current dataset is due to the implicit signal of aerosol trends in the MORECS sunshine duration, although this is likely to be small compared to the effects of changing cloud cover.

The trends in the MORECS sunshine duration used in this study are consistent with changing weather patterns which may be attributed to the Atlantic Multidecadal Oscillation (AMO). The AMO has been shown to cause a decrease in spring precipitation (and therefore cloud cover) in northern Europe over recent decades ~~(Sutton and Dong, 2012)~~(Sutton and Dong, 2012), and the trend in MORECS sunshine hours is dominated by an increase in the spring mean. This has also been seen in Europe-wide sunshine hours data ~~(Sanchez-Lorenzo et al., 2008).~~(Sanchez-Lorenzo et al., 2008). On the other hand, the effect of changing aerosols on sunshine hours is expected to be largest in the winter ~~(Sanchez-Lorenzo et al., 2008)~~(Sanchez-Lorenzo et al., 2008). However, it would not be possible to directly identify either of these effects on the sunshine duration without access to longer data records.

The inclusion of explicit aerosol effects in the coefficients of the Angstrom-Prescott equation would be expected to ~~mitigate the trend in evaporative demand in the first two decades of the dataset, and enhance it after 1980. Gedney et al. (2014)~~reduce the positive trend in AED in the first two decades of the dataset, and increase it after 1980. Gedney et al. (2014) attribute a decrease in European solar radiation of 10 W m^{-2} between the periods 1901-10 and 1974-80, and an increase of 4 W m^{-2} from 1974-84 to1990-99 to changing aerosol contributions. Applying these trends to the current dataset, with a turning point at 1980, would double the overall increase in solar radiation in Great Britain, which would lead to a ~~50~~40 % increase in the overall trend in PET. So, if this effect were to be included, it would confirm the results found in this paper.

~~The trends~~Trends in temperature and cloud cover in the UK are expected to continue into the coming decades, with precipitation expected to increase in the winter but decrease in the summer ~~(Murphy et al., 2009).~~(Murphy et al., 2009). Therefore it is likely that ~~evaporative demand~~AED will increase, increasing water stress in the summer when precipitation is lower and potentially affecting water resources, agriculture and biodiversity. This has been demonstrated for southern England and Wales by ~~Rudd and Kay (2015),~~Rudd and Kay (2015), who calculated present and future PET using high-resolution RCM output and include the effects of CO_2 ~~fertilisation~~on stomatal opening.

The current study is concerned only with the effects of changing climate on ~~evaporative demand~~AED and has assumed a constant bulk canopy resistance throughout. However, plants are expected to react to increased CO_2 in the atmosphere by closing stomata and limiting the exchange of gases, including water ~~(Kruijt et al., 2008)~~(Kruijt et al., 2008), and observed changes in runoff have been attributed to this effect ~~(Gedney et al., 2006; Gedney et al., 2014)~~(Gedney et al., 2006; Gedney et al., 2014). It is possible that the resulting change of canopy resistance could partially offset the increased atmospheric demand ~~(Rudd and Kay, 2015)~~(Rudd and Kay, 2015) and may impact runoff ~~(Gedney et al., 2006; Prudhomme et al., 2014)~~(Gedney et al., 2006; Prudhomme et al., 2014), but further studies would be required to quantify this.

6 Conclusion

This paper has presented a unique high-resolution observation-based dataset of meteorological variables and ~~evaporative demand in Great Britain since 1961. We have shown that trends in evaporative demand can be attributed to trends in the meteorological variables. The~~

~~meteorological variables provided are sufficient to run land surface models and the potential evaporation combined with the potential evaporation can be used to run hydrological models. In addition, the high spatial (1km~~AED in Great Britain since 1961. Key trends in the meteorological variables are (i) increasing air temperature and specific humidity, consistent with global temperature trends; (ii) increasing solar radiation, particularly in the spring, consistent with changes in aerosol emissions and weather patterns in recent decades; (iii) decreasing wind speed, consistent with observations of global stilling; and (iv) increasing precipitation, driven by increasing winter precipitation in Scotland. The meteorological variables were used to evaluate AED in Great Britain via calculation of PET and PETI. It has been demonstrated that including the interception component in the calculation of PETI gives a mean estimate that is overall 8% larger than PET alone, with strong seasonality and spatial variation of the difference. PET was found to be increasing by 0.021±0.021 mm d^{-1} $decade^{-1}$ over the study period. With the interception component included, the trend in PETI is weaker, and over GB is not significant at the 5% level. The trend in PET was analytically attributed to the trends in the meteorological variables, and it was found that the dominant effect was that increasing air temperature was driving increasing PET. This is largely compensated by the associated increase in specific humidity, as the water cycle is intensified under climate change and by decreasing wind speed. However, the PET increase is also driven by increasing solar radiation, particularly in the spring.

In addition to providing meteorological data for analysis, the meteorological variables provided are sufficient to run LSMs and hydrological models. The high spatial (1 km) and temporal (daily) resolution will allow this dataset to be used to study the effects of climate on physical and biological systems at a range of scales, from local to national.

Data Access

The data can be downloaded from the Environmental Information Platform at the Centre for Ecology & Hydrology. The meteorological variables can be found at https://catalogue.ceh.ac.uk/documents/80887755-1426-4dab-a4a6-250919d5020c, while the PET and PETI can be accessed at https://catalogue.ceh.ac.uk/documents/d329f4d6-95ba-4134-b77a-a377e0755653.

Author contribution

EB, JF and DBC designed the study. JF, ACR, DBC and ELR developed code to create meteorological data. ELR created the PET and PETI. ELR and EB analysed trends. ELR, EB, ACR and DBC wrote the manuscript.

Acknowledgements

The meteorological variables presented are based largely on GB meteorological data under licence from the Met Office, and those organisations contributing to this national dataset (including the Met Office, Environment Agency, Scottish Environment Protection Agency (SEPA) and Natural Resources Wales) are gratefully acknowledged. The CRU TS 3.21 daily temperature range data were created by the University of East Anglia Climatic Research Unit, and the WFD air pressure data were created as part of the EU FP6 project WATCH (Contract 036946). Collection of flux data was funded by EU FP4 EuroFlux (Griffin Forest); EU FP5 CarboEuroFlux (Griffin Forest); EU FP5 GreenGrass (Easter Bush); EU FP6 CarboEuropeIP (Alice Holt , Griffin Forest, Auchencorth Moss, Easter Bush); EU FP6 IMECC (Griffin Forest); the Forestry Commission (Alice Holt); the Natural Environment Research Council, UK (Auchencorth Moss, Easter Bush).

Thanks to Nicola Gedney and Graham Weedon for useful discussions.

This work was partially funded by the Natural Environment Research Council in the Changing Water Cycle programme: NERC Reference: NE/I006087/1.

Appendix A: Data validation

Meteorological data were downloaded from the European Fluxes Database Cluster (http://gaia.agraria.unitus.it) for four sites positioned around Great Britain. Two were woodland sites (Alice Holt (Wilkinson et al., 2012; Heinemeyer et al., 2012) and Griffin Forest (Clement, 2003)), while two had grass and crop cover (Auchencorth Moss (Billett et al., 2004) and Easter Bush (Gilmanov et al., 2007; Soussana et al., 2007)). Table A1 gives details of the data used. The data are provided as half-hourly measurements, which were used to create daily means, where full daily data coverage was available. The daily means of the observed data were compared to the daily data from the grid square containing the site and the Pearson correlation (r^2), mean bias and root mean square error (RMSE) were calculated. For each site, monthly means were calculated where the full month had available data, then a climatology calculated from available months. The same values were calculated from the relevant grid squares, using only time periods for which observed data were available.

Fig. A1 shows the comparison of the data set downward SW radiation against daily mean air temperature observed at the four sites. Fig. A2 shows the mean-monthly climatology of the daily values. The observed values of the mixing ratio of water vapour in air were compared with values calculated from the meteorological dataset, using the equation

$$r_w = q_a \left(\frac{m_a}{m_w} \right)$$

where m_a is the molecular mass of dry air and m_w is the molecular mass of water. The comparisons are shown in Figs. A3 and A4.

Table A2 shows the r^2, mean bias and RMSE for each of the variables included in the validation exercise. The correlations indicate a good relationship between the dataset variables and the independent observations at the sites, while the mean-monthly climatologies demonstrate that the data represent the seasonal cycle well.

Appendix B: Trend maps

Fig. B1 shows the rate of change of each of the meteorological variables at the 1 km resolution, while Fig. B2 shows the rate of change of the PET, PETI, and the two components of PET at the same resolution. This shows that the regional trends are consistent with spatial variation and are not dominated by individual extreme points.

Appendix C: Derivatives of ~~potential evaporation~~PET

The wind speed affects the PET through the aerodynamic resistance. The derivative with respect to wind speed is

$$\frac{\partial E_P}{\partial u_{10}} = \frac{(\Delta+\gamma)E_{PA} - \gamma\frac{r_s}{r_a}E_{PR}}{u_{10}\left(\Delta+\gamma\left(1+\frac{r_s}{r_a}\right)\right)} .$$

(~~A1~~C1)

The downward ~~long~~ LW and ~~shortwave~~SW radiation affect PET through the net radiation, and the derivatives are

$$\frac{\partial E_P}{\partial L_d} = E_{PR}\frac{\epsilon}{R_n}$$

(~~A2~~C2)

$$\frac{\partial E_P}{\partial S_d} = E_{PR}\frac{(1-\alpha)}{R_n} .$$

(~~A3~~C3)

The derivative of PET with respect to specific humidity is

$$\frac{\partial E_P}{\partial q_a} = \frac{E_{PA}}{q_a - q_s} .$$

(~~A4~~C4)

The air temperature affects PET through the saturated specific humidity and its derivative, the net radiation and the air density, so that the derivative of PET with respect to air temperature is

$$\frac{\partial E_P}{\partial T_a} = E_{PR}\left(\frac{\gamma\left(1+\frac{r_s}{r_a}\right)}{T_a^2\left(\Delta+\gamma\left(1+\frac{r_s}{r_a}\right)\right)}\left[T_{sp}\left(\sum_{i=1}^{4} i a_i T_r^{i-1} + \frac{\sum_{i=1}^{4} i a_i T_r^{i-1}}{\sum_{i=1}^{4} i(i-1) a_i T_r^{i-2}} + \frac{2(1-\varepsilon)\sum_{i=1}^{4} i a_i T_r^{i-1} q_s}{\varepsilon}\right) - 2T_a\right] - \frac{4\epsilon\sigma T_a^4}{R_n}\right) + E_{PA}\left(\frac{\Delta}{q_s - q} - \frac{1}{T_a} - \frac{\Delta}{T_a^2\left(\Delta+\gamma\left(1+\frac{r_s}{r_a}\right)\right)}\left[T_{sp}\left(\sum_{i=1}^{4} i a_i T_r^{i-1} + \frac{\sum_{i=1}^{4} i a_i T_r^{i-1}}{\sum_{i=1}^{4} i(i-1) a_i T_r^{i-2}} + \frac{2(1-\varepsilon)\sum_{i=1}^{4} i a_i T_r^{i-1} q_s}{\varepsilon}\right) - 2T_a\right]\right) .$$

(~~A5~~)

C5)

~~6~~7 References

Allen, R. G., Pereira, L. S., Raes, D., and Smith, M.: Crop evapotranspiration - Guidelines for computing crop water requirements, Food and Agriculture Organization of the United Nations, Rome, Italy, FAO Irrigation and Drainage Paper, 1998.

Allen, R. G., Trezza, R., and Tasumi, M.: Analytical integrated functions for daily solar radiation on slopes, ~~Agricultural and~~Agr Forest ~~Meteorology~~Meteorol, 139, 55-73, doi:10.1016/j.agrformet.2006.05.012, 2006.

Andréassian, V., Mander, Ü., and Pae, T.: The Budyko hypothesis before Budyko: The hydrological legacy of Evald Oldekop, Journal of Hydrology, 535, 386-391, http://dx.doi.org/10.1016/j.jhydrol.2016.02.002, 2016.

Ångström, A.: A study of the radiation of the atmosphere, Smithsonian Miscellaneous Collections, 65, 159-161, 1918.

Azizzadeh, M., and Javan, K.: Analyzing Trends in Reference Evapotranspiration in Northwest Part of Iran, Journal of Ecological Engineering, 16, 1-12, 10.12911/22998993/1853, 2015.

Baldocchi, D., Valentini, R., Running, S., Oechel, W., and Dahlman, R.: Strategies for measuring and modelling carbon dioxide and water vapour fluxes over terrestrial ecosystems, Global Change Biology, 2, 159-168, doi:10.1111/j.1365-2486.1996.tb00069.x, 1996.

~~Barton, B. T.: Reduced wind strengthens top-down control of an insect herbivore, Ecology, 95, 2375-2381, doi:10.1890/13-2171.1, 2014.~~

Bell, V. A., Kay, A. L., Jones, R. G., Moore, R. J., and Reynard, N. S.: Use of soil data in a grid-based hydrological model to estimate spatial variation in changing flood risk across the UK, Journal of Hydrology, 377, 335-350, doi:10.1016/j.jhydrol.2009.08.031, 2009.

Bell, V. A., Gedney, N., Kay, A. L., Smith, R. N. B., Jones, R. G., and Moore, R. J.: Estimating Potential Evaporation from Vegetated Surfaces for Water Management Impact Assessments Using Climate Model Output, ~~J Hydrometeorol~~Journal of Hydrometeorology, 12, 1127-1136, doi:10.1175/2011jhm1379.1, 2011.

Bell, V. A., Kay, A. L., Cole, S. J., Jones, R. G., Moore, R. J., and Reynard, N. S.: How might climate change affect river flows across the Thames Basin? An area-wide analysis using the UKCP09 Regional Climate Model ensemble, Journal of Hydrology, 442-443, 89-104, doi:10.1016/j.jhydrol.2012.04.001, 2012.

Bellamy, P. H., Loveland, P. J., Bradley, R. I., Lark, R. M., and Kirk, G. J.: Carbon losses from all soils across England and Wales 1978-2003, Nature, 437, 245-248, doi:10.1038/nature04038, 2005.

Berry, P. M., Dawson, T. P., Harrison, P. A., and Pearson, R. G.: Modelling potential impacts of climate change on the bioclimatic envelope of species in Britain and Ireland, Global ~~Ecology and Biogeography~~Ecol Biogeogr, 11, 453-462, doi:~~0~~10.1046/j.1466-822x.2002.00304.x, 2002.

Best, M. J., Pryor, M., Clark, D. B., Rooney, G. G., Essery, R. L. H., Ménard, C. B., Edwards, J. M., Hendry, M. A., Porson, A., Gedney, N., Mercado, L. M., Sitch, S., Blyth, E., Boucher, O., Cox, P. M., Grimmond, C. S. B., and Harding, R. J.: The Joint UK Land Environment

Simulator (JULES), model description – Part 1: Energy and water fluxes, Geoscientific Model Development, 4, 677-699, doi:10.5194/gmd-4-677-2011, 2011.

~~Brittain, C., Kremen, C., and Klein, A.-M.: Biodiversity buffers pollination from changes in environmental conditions, Global Change Biology, 19, 540-547, doi:10.1111/gcb.12043, 2013.~~

Billett, M. F., Palmer, S. M., Hope, D., Deacon, C., Storeton-West, R., Hargreaves, K. J., Flechard, C., and Fowler, D.: Linking land-atmosphere-stream carbon fluxes in a lowland peatland system, Global Biogeochemical Cycles, 18, n/a-n/a, 10.1029/2003gb002058, 2004.

Bosveld, F. C., and Bouten, W.: Evaluating a Model of Evaporation and Transpiration with Observations in a Partially Wet Douglas-Fir Forest, Boundary-Layer Meteorology, 108, 365-396, 10.1023/a:1024148707239, 2003.

Burch, S. F., and Ravenscroft, F.: Computer modelling of the UK wind energy resource: Final overview report., AEA Industrial Technology, 1992.

Burt, T. P., and Shahgedanova, M.: An historical record of evaporation losses since 1815 calculated using long-term observations from the Radcliffe Meteorological Station, Oxford, England, Journal of Hydrology, 205, 101-111, doi:10.1016/S0022-1694(97)00143-1, 1998.

Clark, D. B., Mercado, L. M., Sitch, S., Jones, C. D., Gedney, N., Best, M. J., Pryor, M., Rooney, G. G., Essery, R. L. H., Blyth, E., Boucher, O., Harding, R. J., Huntingford, C., and Cox, P. M.: The Joint UK Land Environment Simulator (JULES), model description – Part 2: Carbon fluxes and vegetation dynamics, Geoscientific Model Development, 4, 701-722, doi:10.5194/gmd-4-701-2011, 2011.

Clement, R. M., J.B.; Jarvis, P.G.: Net carbon productivity of Sitka Spruce forest in Scotland, Scottish Forestry, 5-10, 2003.

Cowley, J. P.: The distribution over Great Britain of global solar irradiation on a horizontal surface, Meteorological Magazine, 107, 357-372, 1978.

Crane, S. B., and Hudson, J. A.: The impact of site factors and climate variability on the calculation of potential evaporation at Moel Cynnedd, Plynlimon, Hydrol. Earth Syst. Sci., 1, 429-445, doi:10.5194/hess-1-429-1997, 1997.

Crooks, S. M., and Naden, P. S.: CLASSIC: a semi-distributed rainfall-runoff modelling system, Hydrol. Earth Syst. Sci., 11, 516-531, doi:10.5194/hess-11-516-2007, 2007.

Crooks, S. M., and Kay, A. L.: Simulation of river flow in the Thames over 120 years: Evidence of change in rainfall-runoff response?, Journal of Hydrology: Regional Studies, 4, Part B, 172-195, doi:10.1016/j.ejrh.2015.05.014, 2015.

Dilley, A. C., and O'Brien, D. M.: Estimating downward clear sky long-wave irradiance at the surface from screen temperature and precipitable water, Quarterly Journal of the Royal Meteorological Society, 124, 1391-1401, doi:10.1256/Smsqj.54902, 1998.

Donohue, R. J., McVicar, T. R., and Roderick, M. L.: Assessing the ability of potential evaporation formulations to capture the dynamics in evaporative demand within a changing climate, Journal of Hydrology, 386, 186-197, doi:10.1016/j.jhydrol.2010.03.020, 2010.

Doorenbos, J. a. P., W. O.: Crop water requirements. FAO Irrigation and Drainage Paper 24., FAO, Rome, Italy, 1977.

Evans, N., Baierl, A., Semenov, M. A., Gladders, P., and Fitt, B. D.: Range and severity of a plant disease increased by global warming, Journal of the Royal Society, Interface / the Royal Society, 5, 525-531, doi:10.1098/rsif.2007.1136, 2008.

FAO/IIASA/ISRIC/ISS-CAS/JRC: Harmonized World Soil Database, 2012.

Fleig, A. K., Tallaksen, L. M., James, P., Hisdal, H., and Stahl, K.: Attribution of European precipitation and temperature trends to changes in synoptic circulation, Hydrology and Earth System Sciences, 19, 3093-3107, 10.5194/hess-19-3093-2015, 2015.

Folland, C. K., Hannaford, J., Bloomfield, J. P., Kendon, M., Svensson, C., Marchant, B. P., Prior, J., and Wallace, E.: Multi-annual droughts in the English Lowlands: a review of their characteristics and climate drivers in the winter half-year, Hydrology and Earth System Sciences, 19, 2353-2375, doi:10.5194/hess-19-2353-2015, 2015.

Gedney, N., Cox, P. M., Betts, R. A., Boucher, O., Huntingford, C., and Stott, P. A.: Detection of a direct carbon dioxide effect in continental river runoff records, Nature, 439, 835-838, doi:10.1038/nature04504, 2006.

Gedney, N., Huntingford, C., Weedon, G. P., Bellouin, N., Boucher, O., and Cox, P. M.: Detection of solar dimming and brightening effects on Northern Hemisphere river flow, ~~Nat Geosci~~Nature Geoscience, 7, 796-800, doi:10.1038/ngeo2263, 2014.

Gill, A. E.: Atmosphere-ocean Dynamics, Academic Press, San Diego, California, USA, 1982.

Gilmanov, T. G., Soussana, J. F., Aires, L., Allard, V., Ammann, C., Balzarolo, M., Barcza, Z., Bernhofer, C., Campbell, C. L., Cernusca, A., Cescatti, A., Clifton-Brown, J., Dirks, B. O. M., Dore, S., Eugster, W., Fuhrer, J., Gimeno, C., Gruenwald, T., Haszpra, L., Hensen, A., Ibrom, A., Jacobs, A. F. G., Jones, M. B., Lanigan, G., Laurila, T., Lohila, A., G.Manca, Marcolla, B., Nagy, Z., Pilegaard, K., Pinter, K., Pio, C., Raschi, A., Rogiers, N., Sanz, M. J., Stefani, P., Sutton, M., Tuba, Z., Valentini, R., Williams, M. L., and Wohlfahrt, G.: Partitioning European grassland net ecosystem CO2 exchange into gross primary productivity and ecosystem respiration using light response function analysis, Agriculture, Ecosystems & Environment, 121, 93-120, 10.1016/j.agee.2006.12.008, 2007.

Gocic, M., and Trajkovic, S.: Analysis of trends in reference evapotranspiration data in a humid climate, Hydrological Sciences Journal, 59, 165-180, 10.1080/02626667.2013.798659, 2013.

Gold, C. M.: Surface interpolation, spatial adjacency and GIS, in: Three Dimensional Applications in Geographical Information Systems, edited by: Raper, J., Taylor and Francis, London, 1989.

Haddeland, I., Clark, D. B., Franssen, W., Ludwig, F., Voß, F., Arnell, N. W., Bertrand, N., Best, M., Folwell, S., Gerten, D., Gomes, S., Gosling, S. N., Hagemann, S., Hanasaki, N., Harding, R., Heinke, J., Kabat, P., Koirala, S., Oki, T., Polcher, J., Stacke, T., Viterbo, P., Weedon, G. P., and Yeh, P.: Multimodel Estimate of the Global Terrestrial Water Balance: Setup and First Results, Journal of Hydrometeorology, 12, 869-884, 10.1175/2011jhm1324.1, 2011.

Hannaford, J., and Buys, G.: Trends in seasonal river flow regimes in the UK, Journal of Hydrology, 475, 158-174, doi:10.1016/j.jhydrol.2012.09.044, 2012.

Hannaford, J.: Climate-driven changes in UK river flows: A review of the evidence, Progress in Physical Geography, 39, 29-48, doi:10.1177/0309133314536755, 2015.

Harris, I., Jones, P. D., Osborn, T. J., and Lister, D. H.: Updated high-resolution grids of monthly climatic observations - the CRU TS3.10 Dataset, International Journal of Climatology, 34, 623-642, ~~Doi~~ doi:10.1002/Joc.3711, 2014.

Hartmann, D. L., Klein Tank, A. M. G., Rusticucci, M., Alexander, L. V., Brönnimann, S., Charabi, Y., Dentener, F. J., Dlugokencky, E. J., Easterling, D. R., Kaplan, A., Soden, B. J., Thorne, P. W., Wild, M., and Zhai, P. M.: Observations: Atmosphere and Surface, in: Climate Change 2013: The Physical Science Basis. Contribution of Working Group I to the Fifth Assessment Report of the Intergovernmental Panel on Climate Change, edited by: Stocker, T. F., Qin, D., Plattner, G.-K., Tignor, M., Allen, S. K., Boschung, J., Nauels, A., Xia, Y., Bex, V., and Midgley, P. M., Cambridge University Press, Cambridge, United Kingdom and New York, NY, USA, 159–254, 2013.

Haslinger, K., and Bartsch, A.: Creating long-term gridded fields of reference evapotranspiration in Alpine terrain based on a recalibrated Hargreaves method, Hydrology and Earth System Sciences, 20, 1211-1223, 10.5194/hess-20-1211-2016, 2016.

Heinemeyer, A., Wilkinson, M., Vargas, R., Subke, J. A., Casella, E., Morison, J. I. L., and Ineson, P.: Exploring the "overflow tap" theory: linking forest soil CO₂ fluxes and individual mycorrhizosphere components to photosynthesis, Biogeosciences, 9, 79-95, 10.5194/bg-9-79-2012, 2012.

Helmes, L., and Jaenicke, R.: Atmospheric turbidity determined from sunshine records, Journal of Aerosol Science, 17, 261-263, doi:10.1016/0021-8502(86)90080-7, 1986.

Hickling, R., Roy, D. B., Hill, J. K., Fox, R., and Thomas, C. D.: The distributions of a wide range of taxonomic groups are expanding polewards, Global Change Biology, 12, 450-455, doi:10.1111/j.1365-2486.2006.01116.x, 2006.

Horn, B. K. P.: Hill Shading and the Reflectance Map, ~~Proceedings of the~~P Ieee, 69, 14-47, doi:10.1109/Proc.1981.11918, 1981.

Hosseinzadeh Talaee, P., Shifteh Some’e, B., and Sobhan Ardakani, S.: Time trend and change point of reference evapotranspiration over Iran, Theoretical and Applied Climatology, 116, 639-647, 10.1007/s00704-013-0978-x, 2013.

Hough, M. N., and Jones, R. J. A.: The United Kingdom Meteorological Office rainfall and evaporation calculation system: MORECS version 2.0-an overview, Hydrology and Earth System Sciences, 1, 227-239, doi:10.5194/hess-1-227-1997, 1997.

IPCC: Climate Change 2013: The Physical Science Basis. Contribution of Working Group I to the Fifth Assessment Report of the Intergovernmental Panel on Climate Change, Cambridge University Press, Cambridge, United Kingdom and New York, NY, USA, 1535 pp., 2013.

IPCC: Climate Change 2014: Impacts, Adaptation, and Vulnerability. Part A: Global and Sectoral Aspects. Contribution of Working Group II to the Fifth Assessment Report of the Intergovernmental Panel on Climate Change [Field, C.B., V.R. Barros, D.J. Dokken, K.J. Mach, M.D. Mastrandrea, T.E. Bilir, M. Chatterjee, K.L. Ebi, Y.O. Estrada, R.C. Genova, B. Girma, E.S. Kissel, A.N. Levy, S. MacCracken, P.R. Mastrandrea, and L.L. White (eds.)], Cambridge University Press, Cambridge, United Kingdom and New York, NY, USA, 1132 pp., 2014a.

IPCC: Climate Change 2014: Impacts, Adaptation, and Vulnerability. Part B: Regional Aspects. Contribution of Working Group II to the Fifth Assessment Report of the Intergovernmental Panel on Climate Change [Barros, V.R., C.B. Field, D.J. Dokken, M.D. Mastrandrea, K.J. Mach, T.E. Bilir, M. Chatterjee, K.L. Ebi, Y.O. Estrada, R.C. Genova, B. Girma, E.S. Kissel, A.N. Levy, S. MacCracken, P.R. Mastrandrea, and L.L. White (eds.)], Cambridge University Press, Cambridge, United Kingdom and New York, NY, USA, 688 pp., 2014b.

Iqbal, M.: An introduction to solar radiation, Academic Press, London, 1983.

Ishibashi, M., and Terashima, I.: Effects of continuous leaf wetness on photosynthesis: adverse aspects of rainfall, Plant, Cell & Environment, 18, 431-438, 10.1111/j.1365-3040.1995.tb00377.x, 1995.

Jenkins, G. J., Perry, M. C., and Prior, M. J.: The climate of the United Kingdom and recent trends, Met Office Hadley Centre, Exeter, UK, 2008.

Jhajharia, D., Dinpashoh, Y., Kahya, E., Singh, V. P., and Fakheri-Fard, A.: Trends in reference evapotranspiration in the humid region of northeast India, Hydrological Processes, 26, 421-435, 10.1002/hyp.8140, 2012.

Jones, P. D., Lister, D. H., Osborn, T. J., Harpham, C., Salmon, M., and Morice, C. P.: Hemispheric and large-scale land-surface air temperature variations: An extensive revision and an update to 2010, Journal of Geophysical Research: Atmospheres, 117, n/a-n/a, doi:10.1029/2011JD017139, 2012.

Jones, P. D., and Harris, I.: CRU TS3.21: Climatic Research Unit (CRU) Time-Series (TS) Version 3.21 of High Resolution Gridded Data of Month-by-month Variation in Climate (Jan. 1901- Dec. 2012). University of East Anglia Climatic Research Unit, doi:10.5285/D0E1585D-3417-485F-87AE-4FCECF10A992, 2013.

Kay, A. L., Bell, V. A., Blyth, E. M., Crooks, S. M., Davies, H. N., and Reynard, N. S.: A hydrological perspective on evaporation: historical trends and future projections in Britain, Journal of Water and Climate Change, 4, 193, doi:10.2166/wcc.2013.014, 2013.

Kay, A. L., Rudd, A. C., Davies, H. N., Kendon, E. J., and Jones, R. G.: Use of very high resolution climate model data for hydrological modelling: baseline performance and future flood changes, Climatic Change, doi:10.1007/s10584-015-1455-6, 2015.

Keller, V. D. J., Tanguy, M., Prosdocimi, I., Terry, J. A., Hitt, O., Cole, S. J., Fry, M., Morris, D. G., and Dixon, H.: CEH-GEAR: 1 km resolution daily and monthly areal rainfall estimates for the UK for hydrological and other applications, Earth Syst. Sci. Data, 7, 143-155, doi:10.5194/essd-7-143-2015, 2015.

Kimball, B. A., Idso, S. B., and Aase, J. K.: A Model of Thermal-Radiation from Partly Cloudy and Overcast Skies, Water Resources Research, 18, 931-936, doi:10.1029/Wr018i004p00931, 1982.

Kruijt, B., Witte, J.-P. M., Jacobs, C. M. J., and Kroon, T.: Effects of rising atmospheric CO2 on evapotranspiration and soil moisture: A practical approach for the Netherlands, Journal of Hydrology, 349, 257-267, doi:10.1016/j.jhydrol.2007.10.052, 2008.

Kume, T., Kuraji, K., Yoshifuji, N., Morooka, T., Sawano, S., Chong, L., and Suzuki, M.: Estimation of canopy drying time after rainfall using sap flow measurements in an emergent tree in a lowland mixed-dipterocarp forest in Sarawak, Malaysia, Hydrological Processes, 20, 565-578, 10.1002/hyp.5924, 2006.

Lange, O. L., Lösch, R., Schulze, E.-D., and Kappen, L.: Responses of stomata to changes in humidity, Planta, 100, 76-86, 10.1007/bf00386887, 1971.

Li, B., Chen, F., and Guo, H.: Regional complexity in trends of potential evapotranspiration and its driving factors in the Upper Mekong River Basin, Quaternary International, 380-381, 83-94, 10.1016/j.quaint.2014.12.052, 2015.

Li, Y., and Zhou, M.: Trends in Dryness Index Based on Potential Evapotranspiration and Precipitation over 1961–2099 in Xinjiang, China, Advances in Meteorology, 2014, 1-15, 10.1155/2014/548230, 2014.

Liley, J. B.: New Zealand dimming and brightening, Journal of Geophysical Research, 114, doi:10.1029/2008jd011401, 2009.

Lu, X., Bai, H., and Mu, X.: Explaining the evaporation paradox in Jiangxi Province of China: Spatial distribution and temporal trends in potential evapotranspiration of Jiangxi Province from 1961 to 2013, International Soil and Water Conservation Research, 4, 45-51, 10.1016/j.iswcr.2016.02.004, 2016.

Marsh, T., and Dixon, H.: The UK water balance – how much has it changed in a warming world?, 01-05, doi:10.7558/bhs.2012.ns32, 2012.

Marthews, T. R., Malhi, Y., and Iwata, H.: Calculating downward longwave radiation under clear and cloudy conditions over a tropical lowland forest site: an evaluation of model schemes for hourly data, Theoretical and Applied Climatology, 107, 461-477, 10.1007/s00704-011-0486-9, 2011.

Matsoukas, C., Benas, N., Hatzianastassiou, N., Pavlakis, K. G., Kanakidou, M., and Vardavas, I.: Potential evaporation trends over land between 1983–2008: driven by radiative fluxes or vapour-pressure deficit?, Atmospheric Chemistry and Physics, 11, 7601-7616, doi:10.5194/acp-11-7601-2011, 2011.

McVicar, T. R., Van Niel, T. G., Li, L. T., Roderick, M. L., Rayner, D. P., Ricciardulli, L., and Donohue, R. J.: Wind speed climatology and trends for Australia, 1975–2006: Capturing the stilling phenomenon and comparison with near-surface reanalysis output, Geophysical Research Letters, 35, n/a-n/a, 10.1029/2008GL035627, 2008.

McVicar, T. R., Roderick, M. L., Donohue, R. J., Li, L. T., Van Niel, T. G., Thomas, A., Grieser, J., Jhajharia, D., Himri, Y., Mahowald, N. M., Mescherskaya, A. V., Kruger, A. C., Rehman, S., and Dinpashoh, Y.: Global review and synthesis of trends in observed terrestrial near-surface wind speeds: Implications for evaporation, Journal of Hydrology, 416, 182-205, doi:10.1016/j.jhydrol.2011.10.024, 2012.

Monteith, J. L.: Evaporation and environment, in: 19th Symposia of the Society for Experimental Biology, University Press, Cambridge, 1965.

Moors, E.: Water Use of Forests in the Netherlands, PhD, Vrije Universiteit, Amsterdam, the Netherlands, 2012.

Morris, D. G., and Flavin, R. W.: A digital terrain model for hydrology~~,~~., Proceedings of the 4th International Symposium on Spatial Data Handling, 1, 250-262, 1990.

Morton, D., Rowland, C., Wood, C., Meek, L., Marston, C., Smith, G., Wadsworth, R., and Simpson, I. C.: Final Report for LCM2007 - the new UK land cover map, NERC/Centre for Ecology & Hydrology 11/07 (CEH Project Number: C03259), 2011.

Muneer, T., and Munawwar, S.: Potential for improvement in estimation of solar diffuse irradiance, ~~Energy Conversion and Management~~Energ Convers Manage, 47, 68-86, doi:10.1016/j.enconman.2005.03.015, 2006.

Murphy, J. M., Sexton, D. M. H., Jenkins, G. J., Boorman, P. M., Booth, B. B. B., Brown, C. C., Clark, R. T., Collins, M., Harris, G. R., Kendon, E. J., Betts, R. A., Brown, S. J., Howard, T. P., Humphrey, K. A., McCarthy, M. P., McDonald, R. E., Stephens, A., Wallace, C., Warren, R., Wilby, R., and Wood, R. A.: UK Climate Projections Science Report: Climate change projections, Met Office Hadley Centre, Exeter, 2009.

Newton, K., and Burch, S. F.: Estimation of the UK wind energy resource using computer modelling techniques and map data, Energy Technology Support Unit, 50, 1985.

Norton, L. R., Maskell, L. C., Smart, S. S., Dunbar, M. J., Emmett, B. A., Carey, P. D., Williams, P., Crowe, A., Chandler, K., Scott, W. A., and Wood, C. M.: Measuring stock and change in the GB countryside for policy--key findings and developments from the Countryside Survey 2007 field survey, Journal of environmental management, 113, 117-127, doi:10.1016/j.jenvman.2012.07.030, 2012.

Oldekop, E.: Evaporation from the surface of river basins, in: Collection of the Works of Students of the Meteorological Observatory, University of Tartu-Jurjew-Dorpat, Tartu, Estonia, 209, 1911.

Palmer, W. C.: Meteorological Drought. Res. Paper No.45, Dept. of Commerce, Washington, D.C., 1965.

Paltineanu, C., Chitu, E., and Mateescu, E.: New trends for reference evapotranspiration and climatic water deficit, International Agrophysics, 26, 10.2478/v10247-012-0023-9, 2012.

Parker, D., and Horton, B.: Uncertainties in central England temperature 1878-2003 and some improvements to the maximum and minimum series, International Journal of Climatology, 25, 1173-1188, doi:10.1002/joc.1190, 2005.

Pocock, M. J., Roy, H. E., Preston, C. D., and Roy, D. B.: The Biological Records Centre in the United Kingdom: a pioneer of citizen science., Biological Journal of the Linnean Society, doi:10.1111/bij.12548, 2015.

Prata, A. J.: A new long-wave formula for estimating downward clear-sky radiation at the surface, Quarterly Journal of the Royal Meteorological Society, 122, 1127-1151, doi:10.1002/qj.49712253306, 1996.

Prescott, J. A.: Evaporation from a water surface in relation to solar radiation, Transaction of the Royal Society of South Australia, 64, 114-125, 1940.

Prudhomme, C., Giuntoli, I., Robinson, E. L., Clark, D. B., Arnell, N. W., Dankers, R., Fekete, B. M., Franssen, W., Gerten, D., Gosling, S. N., Hagemann, S., Hannah, D. M., Kim, H., Masaki, Y., Satoh, Y., Stacke, T., Wada, Y., and Wisser, D.: Hydrological droughts in the 21st century, hotspots and uncertainties from a global multimodel ensemble experiment, Proceedings of the National Academy of Sciences, 111, 3262-3267, doi:10.1073/pnas.1222473110, 2014.

Pryor, S. C., Barthelmie, R. J., Young, D. T., Takle, E. S., Arritt, R. W., Flory, D., Gutowski, W. J., Nunes, A., and Roads, J.: Wind speed trends over the contiguous United States, Journal of Geophysical Research: Atmospheres, 114, n/a-n/a, 10.1029/2008JD011416, 2009.

Reynolds, B., Chamberlain, P. M., Poskitt, J., Woods, C., Scott, W. A., Rowe, E. C., Robinson, D. A., Frogbrook, Z. L., Keith, A. M., Henrys, P. A., Black, H. I. J., and Emmett, B. A.: Countryside Survey: National "Soil Change" 1978–2007 for Topsoils in Great Britain—Acidity, Carbon, and Total Nitrogen Status, Vadose Zone Journal, 12, 0, doi:10.2136/vzj2012.0114, 2013.

Richards, J. M.: A simple expression for the saturation vapour pressure of water in the range −50 to 140°C, Journal of Physics D: Applied Physics, 4, L15, 1971.

Robinson, E. L., Blyth, E., Clark, D. B., Finch, J., and Rudd, A. C.: Climate hydrology and ecology research support system meteorology dataset for Great Britain (1961-2012) [CHESS-met], NERC~~-~~-Environmental Information Data Centre~~, doi:10.5285/80887755-1426-4dab-a4a6-250919d5020c~~, 2015a.

Robinson, E. L., Blyth, E., Clark, D. B., Finch, J., and Rudd, A. C.: Climate hydrology and ecology research support system potential evapotranspiration dataset for Great Britain (1961-2012) [CHESS-PE], NERC~~-~~-Environmental Information Data Centre~~, doi:10.5285/d329f4d6-95ba-4134-b77a-a377e0755653~~, 2015b.

Rodda, J. C., and Marsh, T. J.: The 1975-76 Drought - a contemporary and retrospective review, Wallingford, UK, 2011.

Roderick, M. L., Rotstayn, L. D., Farquhar, G. D., and Hobbins, M. T.: On the attribution of changing pan evaporation, Geophysical Research Letters, 34, 10.1029/2007gl031166, 2007.

Rudd, A. C., and Kay, A. L.: Use of very high resolution climate model data for hydrological modelling: estimation of potential evaporation, Hydrology Research, doi: 10.2166/nh.2015.028, 2015.

Rutter, A. J., Kershaw, K. A., Robins, P. C., and Morton, A. J.: A predictive model of rainfall interception in forests, 1. Derivation of the model from observations in a plantation of Corsican pine, Agricultural Meteorology, 9, 367-384, doi:10.1016/0002-1571(71)90034-3, 1971.

Sanchez-Lorenzo, A., Calbó, J., and Martin-Vide, J.: Spatial and Temporal Trends in Sunshine Duration over Western Europe (1938–2004), Journal of Climate, 21, 6089-6098, doi:10.1175/2008jcli2442.1, 2008.

Sanchez-Lorenzo, A., Calbó, J., Brunetti, M., and Deser, C.: Dimming/brightening over the Iberian Peninsula: Trends in sunshine duration and cloud cover and their relations with atmospheric circulation, Journal of Geophysical Research, 114, doi:10.1029/2008jd011394, 2009.

Sanchez-Lorenzo, A., and Wild, M.: Decadal variations in estimated surface solar radiation over Switzerland since the late 19th century, Atmospheric Chemistry and Physics, 12, 8635-8644, doi:10.5194/acp-12-8635-2012, 2012.

Sanchez-Romero, A., Sanchez-Lorenzo, A., Calbó, J., González, J. A., and Azorin-Molina, C.: The signal of aerosol-induced changes in sunshine duration records: A review of the evidence, Journal of Geophysical Research: Atmospheres, 119, 4657-4673, doi:10.1002/2013JD021393, 2014.

Schymanski, S. J., and Or, D.: Wind effects on leaf transpiration challenge the concept of "potential evaporation", Proceedings of the International Association of Hydrological Sciences, 371, 99-107, 10.5194/piahs-371-99-2015, 2015.

Shan, N., Shi, Z., Yang, X., Zhang, X., Guo, H., Zhang, B., and Zhang, Z.: Trends in potential evapotranspiration from 1960 to 2013 for a desertification-prone region of China, International Journal of Climatology, n/a-n/a, 10.1002/joc.4566, 2015.

Sheffield, J., Goteti, G., and Wood, E. F.: Development of a 50-Year High-Resolution Global Dataset of Meteorological Forcings for Land Surface Modeling, Journal of Climate, 19, 3088-3111, doi:10.1175/JCLI3790.1, 2006.

Shuttleworth, W. J.: Terrestrial Hydrometeorology, John Wiley & Sons, Ltd, 2012.

Sinden, G.: Characteristics of the UK wind resource: Long-term patterns and relationship to electricity demand, Energy Policy, 35, 112-127, doi:10.1016/j.enpol.2005.10.003, 2007.

Song, Z. W. Z., H. L. ; Snyder, R. L. ;Anderson, F. E. ;Chen, F. : Distribution and Trends in Reference Evapotranspiration in the North China Plain, Journal of Irrigation and Drainage Engineering, 136, 240-247, doi:10.1061/(ASCE)IR.1943-4774.0000175, 2010.

Soussana, J. F., Allard, V., Pilegaard, K., Ambus, P., Amman, C., Campbell, C., Ceschia, E., Clifton-Brown, J., Czobel, S., Domingues, R., Flechard, C., Fuhrer, J., Hensen, A., Horvath, L., Jones, M., Kasper, G., Martin, C., Nagy, Z., Neftel, A., Raschi, A., Baronti, S., Rees, R. M., Skiba, U., Stefani, P., Manca, G., Sutton, M., Tuba, Z., and Valentini, R.: Full accounting of the greenhouse gas (CO2, N2O, CH4) budget of nine European grassland sites, Agriculture, Ecosystems & Environment, 121, 121-134, 10.1016/j.agee.2006.12.022, 2007.

Stanhill, G., and Cohen, S.: Solar Radiation Changes in the United States during the Twentieth Century: Evidence from Sunshine Duration Measurements, Journal of Climate, 18, 1503-1512, doi:10.1175/JCLI3354.1, 2005.

Stanhill, G., and Möller, M.: Evaporative climate change in the British Isles, International Journal of Climatology, 28, 1127-1137, doi:10.1002/joc.1619, 2008.

Stewart, J. B.: On the use of the Penman-Monteith equation for determining areal evapotranspiration, in: Estimation of Areal Evapotranspiration (Proceedings of a workshop held at Vancouver, B.C., Canada, August 1987). edited by: Black, T. A. S., D. L.; Novak, M. D.; Price, D. T., IAHS, Wallingford, Oxfordshire, UK, 1989.

Sutton, R. T., and Dong, B.: Atlantic Ocean influence on a shift in European climate in the 1990s, Nature Geosci, 5, 788-792, doi:10.1038/ngeo1595, 2012.

Tabari, H., Nikbakht, J., and Hosseinzadeh Talaee, P.: Identification of Trend in Reference Evapotranspiration Series with Serial Dependence in Iran, Water Resources Management, 26, 2219-2232, 10.1007/s11269-012-0011-7, 2012.

Tanguy, M., Dixon, H., Prosdocimi, I., Morris, D. G., and Keller, V. D. J.: Gridded estimates of daily and monthly areal rainfall for the United Kingdom (1890-2012) [CEH-GEAR], NERC Environmental Information Data Centre, doi:10.5285/5dc179dc-f692-49ba-9326-a6893a503f6e, 2014.

Thackeray, S. J., Sparks, T. H., Frederiksen, M., Burthe, S., Bacon, P. J., Bell, J. R., Botham, M. S., Brereton, T. M., Bright, P. W., Carvalho, L., Clutton-Brock, T., Dawson, A., Edwards, M., Elliott, J. M., Harrington, R., Johns, D., Jones, I. D., Jones, J. T., Leech, D. I., Roy, D. B., Scott, W. A., Smith, M., Smithers, R. J., Winfield, I. J., and Wanless, S.: Trophic level asynchrony in rates of phenological change for marine, freshwater and terrestrial environments, Global Change Biology, 16, 3304-3313, doi:10.1111/j.1365-2486.2010.02165.x, 2010.

Thompson, N., Barrie, I. A., and Ayles, M.: The Meteorological Office rainfall and evaporation calculation system: MORECS, Meteorological Office, Bracknell, 1981.

CRU TS3.21: Climatic Research Unit (CRU) Time-Series (TS) Version 3.21 of High Resolution Gridded Data of Month-by-month Variation in Climate (Jan. 1901- Dec. 2012), 2013.

Vautard, R., Cattiaux, J., Yiou, P., Thepaut, J. N., and Ciais, P.: Northern Hemisphere atmospheric stilling partly attributed to an increase in surface roughness, ~~Nat Geosci~~Nature Geoscience, 3, 756-761, doi:10.1038/Ngeo979, 2010.

Vicente-Serrano, S. M., Azorin-Molina, C., Sanchez-Lorenzo, A., Revuelto, J., López-Moreno, J. I., González-Hidalgo, J. C., Moran-Tejeda, E., and Espejo, F.: Reference evapotranspiration variability and trends in Spain, 1961–2011, Global and Planetary Change, 121, 26-40, 10.1016/j.gloplacha.2014.06.005, 2014.

Vicente-Serrano, S. M., Azorin-Molina, C., Sanchez-Lorenzo, A., El Kenawy, A., Martín-Hernández, N., Peña-Gallardo, M., Beguería, S., and Tomas-Burguera, M.: Recent changes and drivers of the atmospheric evaporative demand in the Canary Islands, Hydrology and Earth System Sciences Discussions, 1-35, 10.5194/hess-2016-15, 2016.

Vincent, L. A., Zhang, X., Brown, R. D., Feng, Y., Mekis, E., Milewska, E. J., Wan, H., and Wang, X. L.: Observed Trends in Canada's Climate and Influence of Low-Frequency Variability Modes, Journal of Climate, 28, 4545-4560, 10.1175/jcli-d-14-00697.1, 2015.

von Storch, H., and Zwiers, F. W.: Statistical analysis in climate research, Cambridge University Press, Cambridge ; New York, x, 484 p. pp., 1999.

Wang, K., and Liang, S.: Global atmospheric downward longwave radiation over land surface under all-sky conditions from 1973 to 2008, Journal of Geophysical Research, 114, doi:10.1029/2009jd011800, 2009.

Ward, R. C., and Robinson, M.: Principles of Hydrology, McGraw Hill, 2000.

Watts, G., Battarbee, R. W., Bloomfield, J. P., Crossman, J., Daccache, A., Durance, I., Elliott, J. A., Garner, G., Hannaford, J., Hannah, D. M., Hess, T., Jackson, C. R., Kay, A. L., Kernan, M., Knox, J., Mackay, J., Monteith, D. T., Ormerod, S. J., Rance, J., Stuart, M. E., Wade, A. J., Wade, S. D., Weatherhead, K., Whitehead, P. G., and Wilby, R. L.: Climate change and water in the UK - past changes and future prospects, Progress in Physical Geography, 39, 6-28, doi:10.1177/0309133314542957, 2015.

Weedon, G. P., Gomes, S., Viterbo, P., Shuttleworth, W. J., Blyth, E., Osterle, H., Adam, J. C., Bellouin, N., Boucher, O., and Best, M.: Creation of the WATCH Forcing Data and Its Use to Assess Global and Regional Reference Crop Evaporation over Land during the Twentieth Century, ~~J Hydrometeorol~~Journal of Hydrometeorology, 12, 823-848, doi:10.1175/2011jhm1369.1, 2011.

Weedon, G. P., Balsamo, G., Bellouin, N., Gomes, S., Best, M. J., and Viterbo, P.: The WFDEI meteorological forcing data set: WATCH Forcing Data methodology applied to ERA-Interim reanalysis data, Water Resources Research, 50, 7505-7514, doi:10.1002/2014WR015638, 2014.

Wild, M.: Global dimming and brightening: A review, Journal of Geophysical Research, 114, doi:10.1029/2008jd011470, 2009.

Wilkinson, M., Eaton, E. L., Broadmeadow, M. S. J., and Morison, J. I. L.: Inter-annual variation of carbon uptake by a plantation oak woodland in south-eastern England, Biogeosciences, 9, 5373-5389, 10.5194/bg-9-5373-2012, 2012.

WMO: Manual on the Global Observing System, Secretariat of the World Meteorological Organization, Geneva, Switzerland, 2013.

Wood, C. M., Smart, S. M., and Bunce, R. G. H.: Woodland survey of Great Britain 1971–2001, Earth System Science Data Discussions, 8, 259-277, doi:10.5194/essdd-8-259-2015, 2015.

Yin, Y., Wu, S., Chen, G., and Dai, E.: Attribution analyses of potential evapotranspiration changes in China since the 1960s, Theoretical and Applied Climatology, 101, 19-28, 10.1007/s00704-009-0197-7, 2009.

Zhang, K.-x., Pan, S.-m., Zhang, W., Xu, Y.-h., Cao, L.-g., Hao, Y.-p., and Wang, Y.: Influence of climate change on reference evapotranspiration and aridity index and their temporal-spatial variations in the Yellow River Basin, China, from 1961 to 2012, Quaternary International, 380-381, 75-82, 10.1016/j.quaint.2014.12.037, 2015.

Zhao, J., Xu, Z.-x., Zuo, D.-p., and Wang, X.-m.: Temporal variations of reference evapotranspiration and its sensitivity to meteorological factors in Heihe River Basin, China, Water Science and Engineering, 8, 1-8, 10.1016/j.wse.2015.01.004, 2015.

Zwiers, F. W., and von Storch, H.: Taking Serial-Correlation into Account in Tests of the Mean, Journal of Climate, 8, 336-351, doi:10.1175/1520-0442(1995)008<0336:Tsciai>2.0.Co;2, 1995.

Table 1. ~~Variable details~~Description of input meteorological variables

Variable (units)	Source data	Ancillary files	Assumptions	Height
Air temperature (K)	MORECS air temperature	IHDTM elevation	Lapsed to IHDTM elevation	1.2 m
Specific humidity (kg kg^{-1})	MORECS vapour pressure, air temperature	IHDTM elevation	Lapsed to IHDTM elevation Constant air pressure	1.2 m
Downward ~~longwave~~LW radiation (W m^{-2})	MORECS air temperature, vapour pressure, sunshine hours	IHDTM elevation	Constant cloud base height	~~n/a~~1.2 m
Downward ~~shortwave~~SW radiation (W m^{-2})	MORECS sunshine hours	IHDTM elevation Spatially-varying aerosol correction	No time-varying aerosol correction	~~n/a~~1.2 m
Wind speed (m s^{-1})	MORECS wind speed	ETSU average wind speeds	Wind speed correction is constant	10 m
Precipitation (kg m^{-2} s^{-1})	CEH-GEAR precipitation	-	No transformations performed	n/a
Daily temperature range (K)	CRU TS 3.21 daily temperature range	-	No spatial interpolation from 0.5° resolution. No temporal interpolation (constant values for each month)	1.2 m

Surface air pressure (Pa)	WFD air pressure	IHDTM elevation	Mean-monthly values from WFD used (each year has same values). Lapsed to IHDTM elevation. No temporal interpolation (constant values for each month).	n/a

Table 2: Rate of change of annual means of meteorological and potential ~~evaptranspiration~~evapotranspiration variables in Great Britain. Bold indicates trends that are significant at the 5% level. The ranges are given by the 95% CI.

Variable		Rate of change ~~(~~± 95% ~~confidence interval)~~CI				
		Great Britain	England	Scotland	Wales	English lowlands
Air temperature (K dec^{-1})		**0.~~20~~ ~~(~~21 ± 0.~~07, 0.31) K decade^{-1}~~15**	**0.23 ± 0.14**	**0.17 ± 0.12**	**0.21 ± 0.15**	**0.25 ± 0.17**
Specific humidity (g kg^{-1} dec^{-1})		**~~0.046 (0.010, 0.082) g kg^{-1} decade^{-1}~~0.049 ± 0.037**	**0.054 ± 0.04**	**0.040 ± 0.036**	**0.055 ± 0.037**	**0.053 ± 0.044**
Downward ~~shortwave~~SW radiation (W m^{-2} dec^{-1})		**1.0 ± 0.8**	**1.3 ± 1 ~~(~~.0.~~3, 1.8) W m^{-2} decade^{-1}~~**	0.5 ± 0.6	**1.1 ± 0.9**	**1.5 ± 1.0**
Downward ~~longwave~~LW radiation (W m^{-2} dec^{-1})		**0.50 ± 0.48**	0.45 ~~(~~± 0.~~01,0.91) W m^{-2} decade^{-1}~~48	**0.58 ± 0.48**	0.50 ± 0.55	0.42 ± 0.48
~~Wind speed~~	~~-0.17 (-0.27, -0.08)~~ Wind speed (m s^{-1} ~~decade~~dec^{-1})	**-0.18 ± 0.09**	**-0.16 ± 0.09**	**-0.20 ± 0.10**	**-0.25 ± 0.16**	**-0.13 ± 0.07**
Precipitation (mm d^{-1} dec^{-1})		**0.08 ~~(~~± 0.~~02, 0.14) mm day^{-1} decade^{-1}~~06**	0.04 ± 0.06	**0.14 ± 0.09**	0.08 ± 0.09	0.03 ± 0.05
Daily temperature range (K dec^{-1})		-0.06 ~~(-~~ ± 0.~~12,0.0~~	-0.03 ± 0.06	**-0.13 ± 0.08**	0.00 ± 0.06	-0.04 ± 0.07

	~~0) K decade^-1^~~06				
PET (mm d^-1^ dec^-1^)	**0.021 ~~(~~± 0.~~00,0.041) mm day^-1^ decade^-1^~~021**	**0.025 ± 0.024**	**0.015 ± 0.015**	0.017 ± 0.021	**0.03 ± 0.026**
Radiative component of PET (mm d^-1^ dec^-1^)	**0.016 ± 0.010**	**0.018 ± 0.011**	**0.013 ± 0.008**	**0.020 ± 0.013**	**0.018 ± 0.011**
Aerodynamic component of PET (mm d^-1^ dec^-1^)	0.007 ± 0.011	0.009 ± 0.013	0.004 ± 0.009	0.001 ± 0.013	0.015 ± 0.015
PETI (mm d^-1^ dec^-1^)	0.019 ~~(~~± 0.~~00,0.039) mm day^-1^ decade^-1^~~020	**0.023 ± 0.023**	0.014 ± 0.014	0.016 ± 0.020	**0.028 ± 0.025**

~~Table 3. Percentage contribution~~

Table 3. Contributions to the rate of change of PET and its radiative and aerodynamic components. For each variable, the first column shows the contribution calculated using regional averages, along with the associated 95% CI. The second column shows the contribution calculated at 1 km resolution, then averaged over each region. The uncertainty on this value is difficult to calculate as the pixels are highly spatially correlated, so the uncertainty range from the regional analysis is used in Fig. 13.

a) Contribution to rate of change of PET (mm d^{-1} $decade^{-1}$)

	Air temperature		Specific humidity		Wind speed		Downward LW		Downward SW		Total	
	Regional	Pixel	Regional	Pixel	Regional	Pixel	Regional	Pixel	Regional	Pixel	Regional	Pixel
England	**0.041 ± 0.025**	0.039	**-0.025 ± 0.019**	-0.024	**-0.010 ± 0.005**	-0.007	0.005 ± 0.006	0.005	**0.013 ± 0.009**	0.012	0.025 ± 0.034	0.024
Scotland	**0.029 ± 0.021**	0.023	**-0.020 ± 0.018**	-0.017	**-0.010 ± 0.005**	-0.007	**0.006 ± 0.005**	0.006	0.005 ± 0.005	0.004	0.010 ± 0.029	0.008
Wales	**0.039 ± 0.028**	0.036	**-0.026 ± 0.018**	-0.025	**-0.011 ± 0.007**	-0.009	0.006 ± 0.006	0.006	**0.010 ± 0.009**	0.009	0.017 ± 0.036	0.017
English lowlands	**0.043 ± 0.029**	0.042	**-0.024 ± 0.020**	-0.023	**-0.008 ± 0.004**	-0.008	0.005 ± 0.006	0.005	**0.015 ± 0.010**	0.015	0.031 ± 0.038	0.030
Great Britain	**0.037 ± 0.026**	0.031	**-0.023 ± 0.018**	-0.022	**-0.010 ± 0.005**	-0.007	**0.006 ± 0.005**	0.005	**0.010 ± 0.007**	0.007	0.019 ± 0.033	0.014

b) Contribution to rate of change of radiative component of (mm d^{-1} $decade^{-1}$)

	Air temperature		Specific humidity		Wind speed		Downward LW		Downward SW		Total	
	Regional	Pixel	Regional	Pixel	Regional	Pixel	Regional	Pixel	Regional	Pixel	Regional	Pixel
England	**-0.009 ± 0.006**	-0.009	n/a	n/a	**0.009 ± 0.005**	0.007	0.005 ± 0.006	0.005	**0.014 ± 0.010**	0.013	**0.018 ± 0.013**	0.016
Scotland	**-0.006 ± 0.005**	-0.006	n/a	n/a	**0.009 ± 0.004**	0.007	**0.006 ± 0.005**	0.006	0.005 ± 0.005	0.004	**0.014 ± 0.010**	0.012
Wales	**-0.007 ± 0.005**	-0.007	n/a	n/a	**0.014 ± 0.009**	0.013	0.006 ± 0.006	0.006	**0.010 ± 0.009**	0.010	**0.023 ± 0.015**	0.022
English lowlands	**-0.010 ± 0.007**	-0.010	n/a	n/a	**0.007 ± 0.004**	0.006	0.005 ± 0.006	0.005	**0.016 ± 0.011**	0.015	**0.017 ± 0.014**	0.017
Great Britain	**-0.008 ± 0.006**	-0.007	n/a	n/a	**0.009 ± 0.005**	0.007	**0.006 ± 0.006**	0.006	**0.010 ± 0.008**	0.008	**0.017 ± 0.012**	0.013

c) Contribution to rate of change of aerodynamic component of PET (mm d^{-1} $decade^{-1}$)

	Air temperature		Specific humidity		Wind speed		Downward LW		Downward SW		Total	
	Regional	Pixel	Regional	Pixel	Regional	Pixel	Regional	Pixel	Regional	Pixel	Regional	Pixel

England	**0.052 ± 0.032**	0.050	**-0.026 ± 0.020**	-0.026	**-0.018 ± 0.010**	-0.015	n/a	n/a	n/a	n/a	0.007 ± 0.039	0.009
Scotland	**0.037 ± 0.027**	0.033	**-0.021 ± 0.019**	-0.019	**-0.019 ± 0.010**	-0.015	n/a	n/a	n/a	n/a	-0.003 ± 0.034	-0.001
Wales	**0.048 ± 0.035**	0.046	**-0.028 ± 0.019**	-0.027	**-0.026 ± 0.016**	-0.023	n/a	n/a	n/a	n/a	-0.005 ± 0.042	-0.003
English lowlands	**0.056 ± 0.037**	0.055	**-0.026 ± 0.021**	-0.025	**-0.015 ± 0.008**	-0.014	n/a	n/a	n/a	n/a	0.015 ± 0.044	0.015
Great Britain	**0.046 ± 0.033**	0.041	**-0.025 ± 0.019**	-0.023	**-0.020 ± 0.010**	-0.015	n/a	n/a	n/a	n/a	0.002 ± 0.039	0.003

Table 4. Contribution of the trend in each variable to the trends in annual mean PET and its radiative and aerodynamic components. as a percentage of the fitted trend in PET and its components.

a) Potential evapotranspiration (PET)						
	Air temperature	Specific humidity	Wind speed	Downward longwaveLW	Downward shortwaveSW	Total
England	7.7154 %	-4.688 %	-1.822 %	26.417 %	72.347 %	108 %
Scotland	9.2150 %	-6.074 %	-3.223 %	53.426 %	46.518 %	97 %
Wales	8.2200 %	-5.6130 %	-2.438 %	32.728 %	67.050 %	109 %
English lowlands	7.3142 %	-4.077 %	-1.420 %	22.715 %	75.345 %	105 %
Great Britain	8.1155 %	-5.187 %	-2.223 %	33.919 %	65.331 %	96 %

b) Radiative component of PET						
	Air temperature	Specific humidity	Wind speed	Downward longwaveLW	Downward shortwaveSW	Total
England	-1.647 %	n/a	1.540 %	26.828 %	73.371 %	92 %
Scotland	-1.942 %	n/a	2.562 53.1 % %	46.3 %	36 %	102 %
Wales	-1.534 %	n/a	2.869 %	32.329 %	66.352 %	116 %
English lowlands	-1.753 %	n/a	1.135 %	23.327 %	77.286 %	95 %
Great Britain	-1.744 %	n/a	1.946 %	34.131 %	65.753 %	87 %

c) Aerodynamic component of PET						
	Air temperature	Specific humidity	Wind speed	Downward longwaveLW	Downward shortwaveSW	Total
England	703.7245 %	-353.5115 %	-250.248 %	n/a	n/a	82 %
Scotland	-1210.068 %	662.2-14 %	647.3-33 %	n/a	n/a	21 %
Wales	-854.7135 %	492.372 %	462.5-42 %	n/a	n/a	-105 %
English lowlands	365.4282 %	-165.8126 %	-99.647 %	n/a	n/a	109 %
Great Britain	2025.0168 %	-1061.976 %	-863.144 %	n/a	n/a	48 %

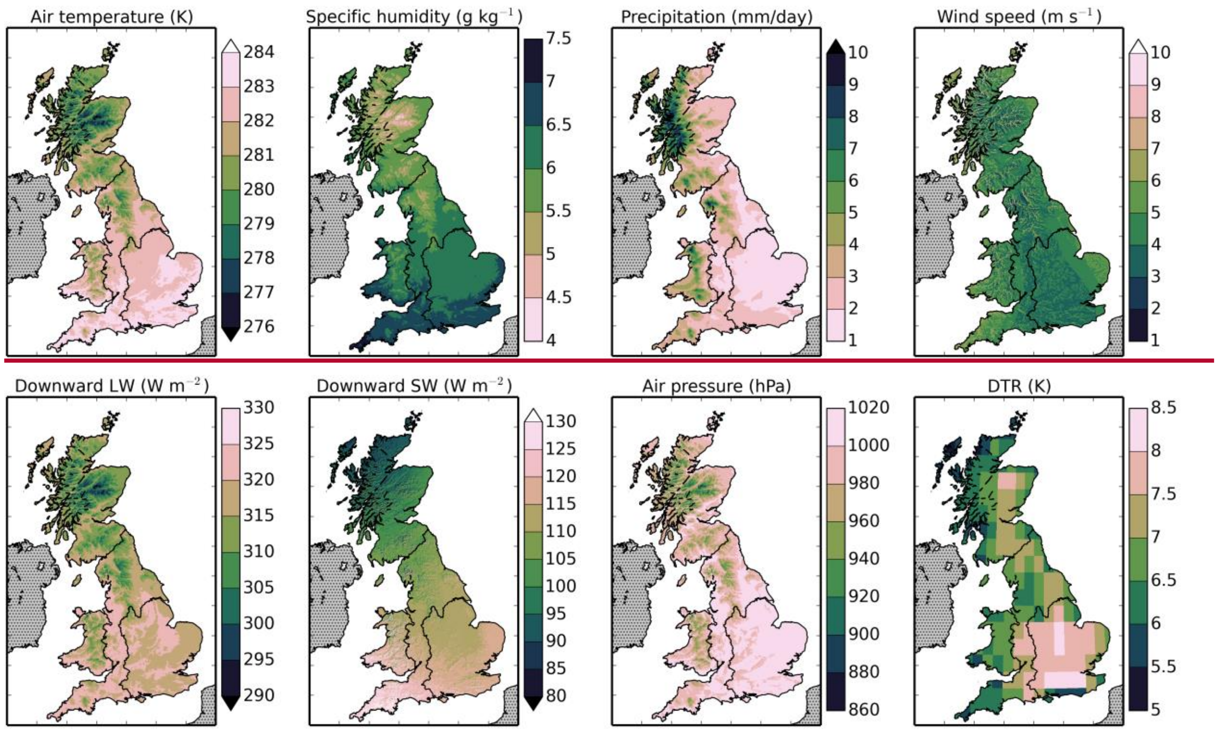
Air temperature (K)
284 283 282 281 280 279 278 277 276
Specific humidity (g kg^{-1})
7.5 7 6.5 6 5.5 5 4.5 4
Precipitation (mm/day)
10 9 8 7 6 5 4 3 2 1
Wind speed (m s^{-1})
10 9 8 7 6 5 4 3 2 1
Downward LW (W m^{-2})
330 325 320 315 310 305 300 295 290
Downward SW (W m^{-2})
130 125 120 115 110 105 100 95 90 85 80
Air pressure (hPa)
1020 1000 980 960 940 920 900 880 860
DTR (K)
8.5 8 7.5 7 6.5 6 5.5 5

Table A1. Details of sites used for validation of meteorological data.

Site (ID)	Latitude	Longitude	Years	Land cover	Citation
Alice Holt (UK-Ham)	51.15	-0.86	2004-2012	Deciduous broadleaf woodland	(Wilkinson et al., 2012; Heinemeyer et al., 2012)
Griffin Forest (UK-Gri)	56.61	-3.80	1997-2001, 2004-2008	Evergreen needleleaf woodland	(Clement, 2003)
Auchencorth Moss (UK-AMo)	55.79	-3.24	2002-2006	Grass and crop	(Billett et al., 2004)
Easter Bush (UK-EBu)	55.87	-3.21	2004-2008	Grass	(Gilmanov et al., 2007; Soussana et al., 2007)

Table A2. Correlation statistics for meteorological variables with data from four sites.

a) Air temperature			
Site	r^2	Mean bias	RMSE
Alice Holt	0.95	0.10 K	1.17 K
Griffin Forest	0.94	0.21 K	1.17 K
Auchencorth Moss	0.98	-0.02 K	0.78 K
Easter Bush	0.97	-0.46 K	0.96 K
b) Downward SW radiation			
Site	r^2	Mean bias	RMSE
Alice Holt	0.94	-3.01 W m^{-2}	22.92 W m^{-2}
Griffin Forest	0.85	-4.90 W m^{-2}	31.29 W m^{-2}
Auchencorth Moss	0.91	14.27 W m^{-2}	27.96 W m^{-2}
Easter Bush	0.88	5.73 W m^{-2}	27.15 W m^{-2}
c) Mixing ratio			
Site	r^2	Mean bias	RMSE
Alice Holt	0.90	-0.02 mmol mol^{-1}	1.09 mmol mol^{-1}
Griffin Forest	0.76	0.08 mmol mol^{-1}	1.56 mmol mol^{-1}
d) Wind speed			
Site	r^2	mean bias	RMSE
Alice Holt	0.88	1.24 m s^{-1}	1.45 m s^{-1}
Griffin Forest	0.59	1.36 m s^{-1}	1.81 m s^{-1}
Auchencorth Moss	0.63	-0.38 m s^{-1}	1.37 m s^{-1}
Easter Bush	0.82	0.44 m s^{-1}	1.03 m s^{-1}
e) Surface air pressure			
Site	r^2	Mean bias	RMSE
Griffin Forest	0.05	-0.42 hPa	1.38 hPa
Auchencorth Moss	0.01	-1.06 hPa	1.57 hPa
Easter Bush	0.03	0.01 hPa	1.33 hPa

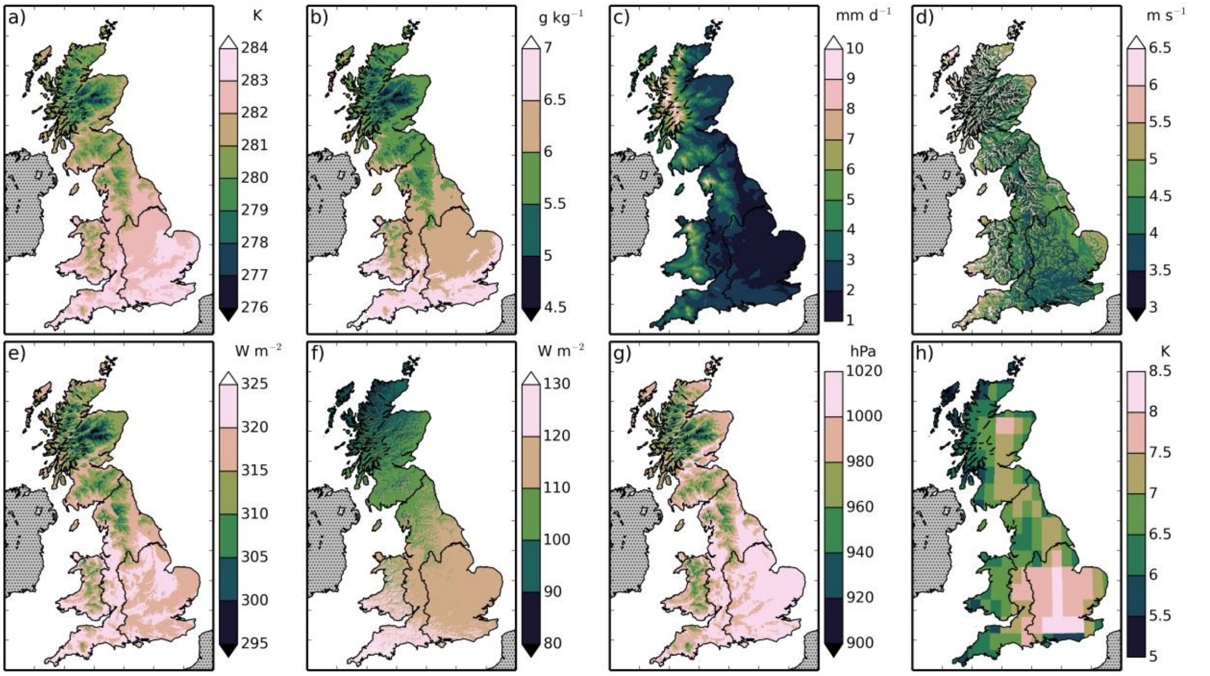

Figure 1. Means of the meteorological variables over the years 1961-2012. ~~Top row, left to right~~The variables are a) 1.2 m air temperature, b) 1.2 m specific humidity, c) precipitation, d) 10 m wind speed~~. Bottom row left to right are~~, e) downward ~~longwave radiation, downward shortwave~~LW radiation, f) downward SW radiation, g) surface air pressure, h) daily air temperature range.

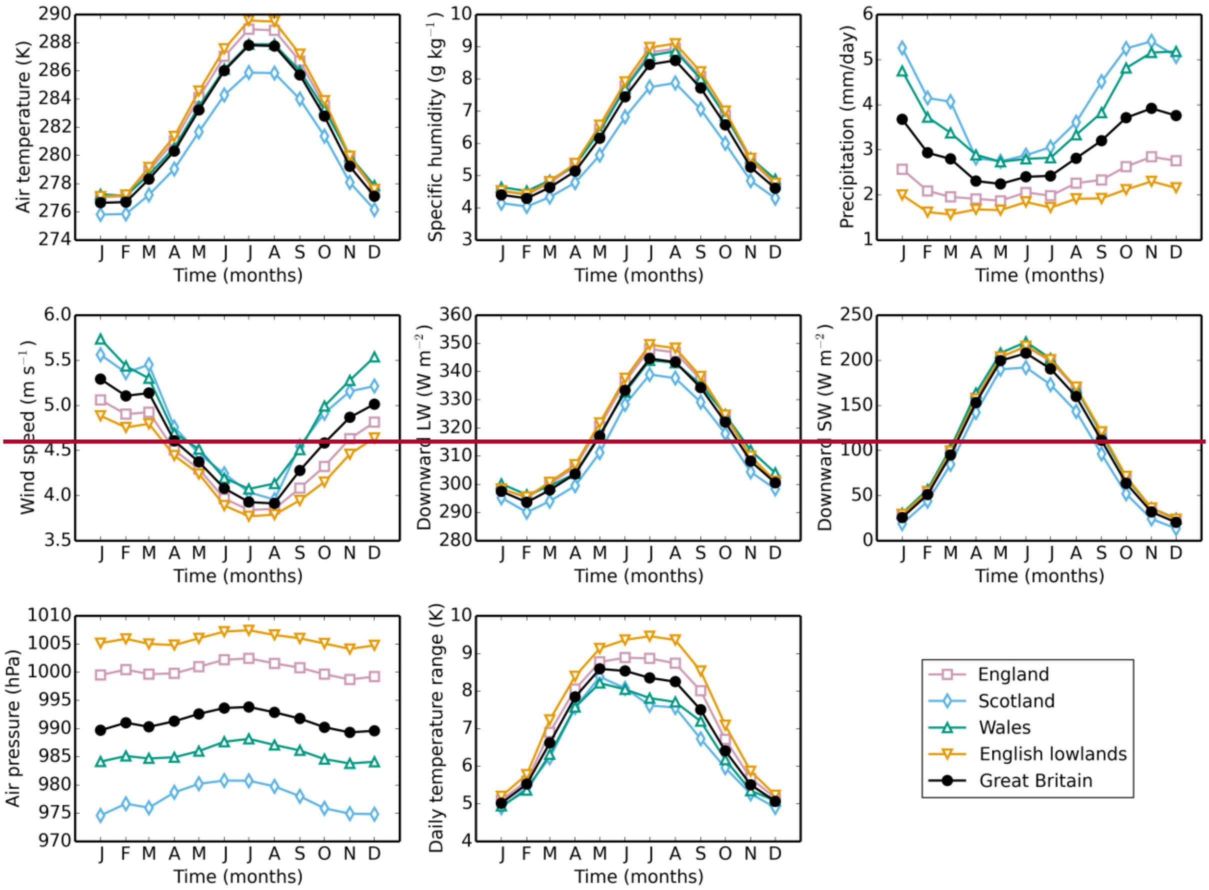

~~Figure 2. Mean monthly climatology of meteorological variables for five different regions of Great Britain, calculated over the years 1961-2012.~~

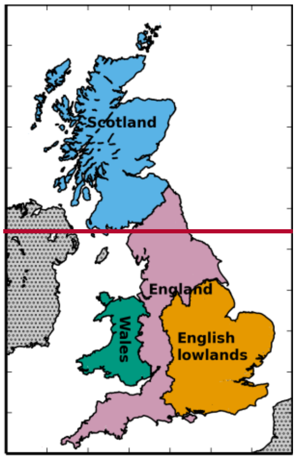

Figure 3.

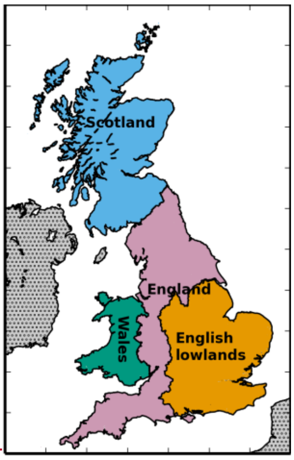

Figure 2. The regions used to calculate the area means. The English lowlands are a sub-region of England. England, Scotland and Wales together form the fifth region, Great Britain.

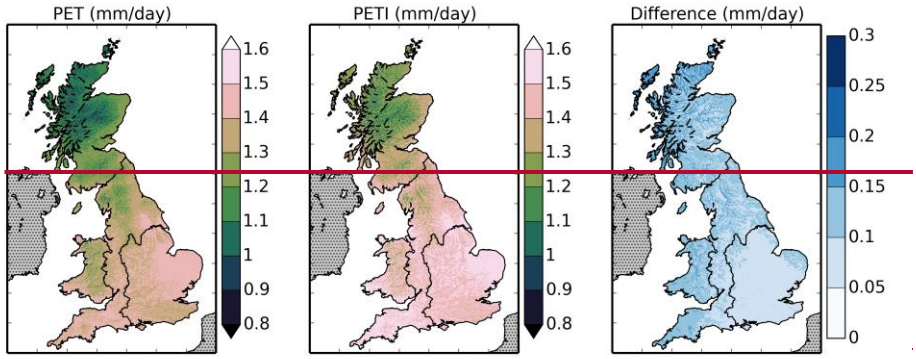

Figure 4. Mean PET (right), mean PETI (centre), and the difference between mean PETI and PET (right), calculated over the years 1961-2012.

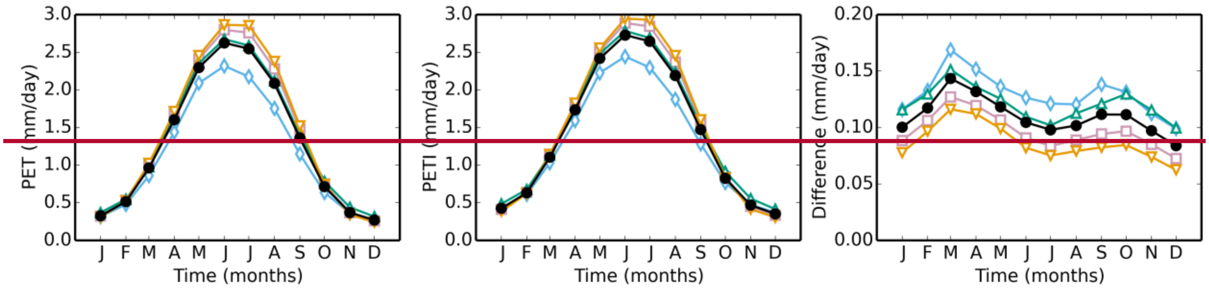

~~Figure 5.~~

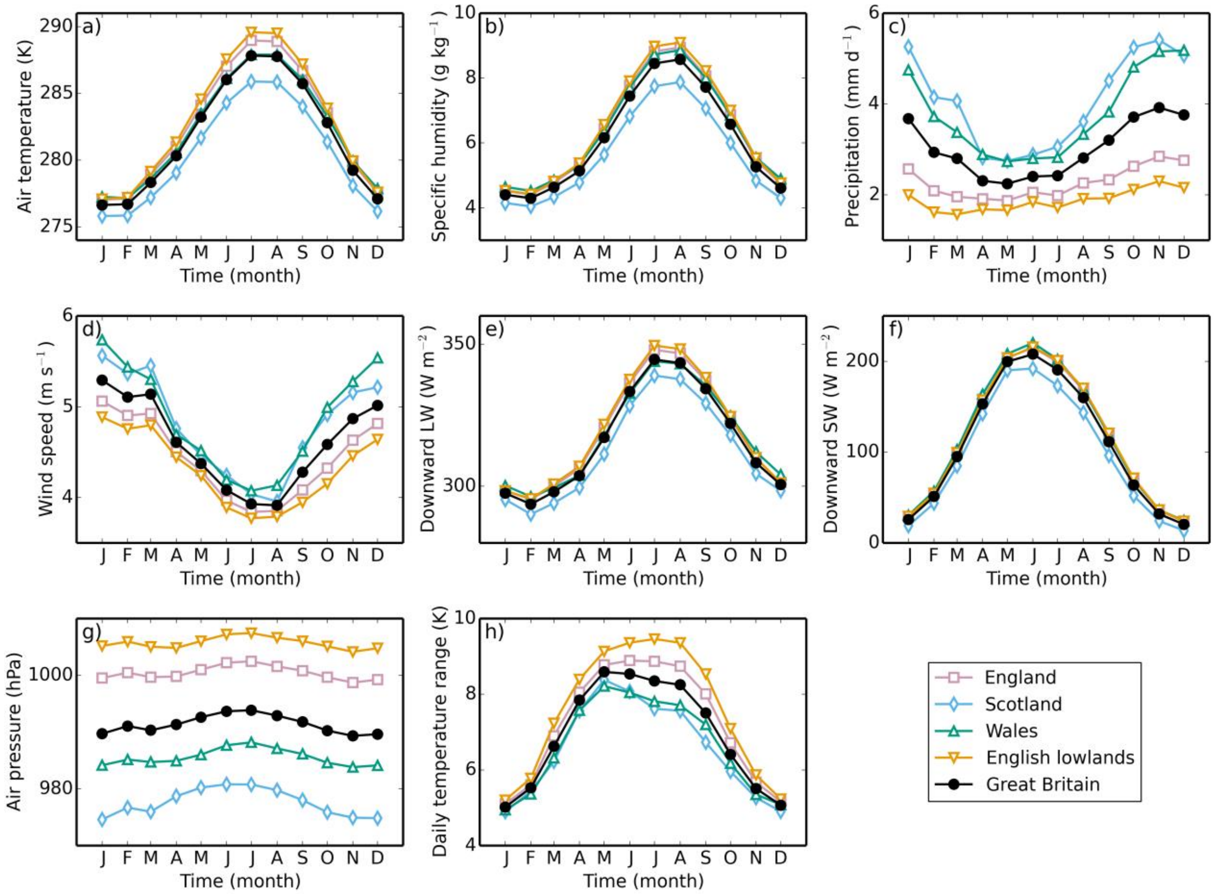

Figure 3. Mean monthly climatology of ~~PET (left), PETI (centre) and the difference PETI-PET (right)~~meteorological variables, a) 1.2 m air temperature, b) 1.2 m specific humidity, c) precipitation, d) 10 m wind speed, e) downward LW radiation, f) downward SW radiation, g) surface air pressure, h) daily air temperature range, for five different regions of Great Britain, calculated over the years 1961-2012.

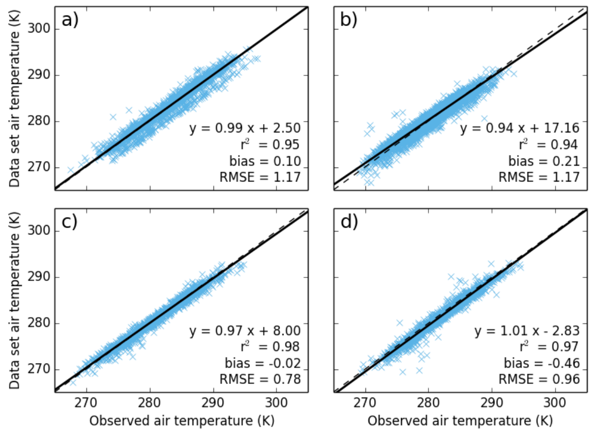

Figure 4. Plot of data set air temperature against daily mean air temperature at four sites. The dashed line shows the one to one line, while the solid line shows the linear regression, the equation of which is shown in the lower right of each plot, along with the r^2 value, the mean bias and the RMSE. The sites are a) Alice Holt; b) Griffin Forest; c) Auchencorth Moss; d) Easter Bush.

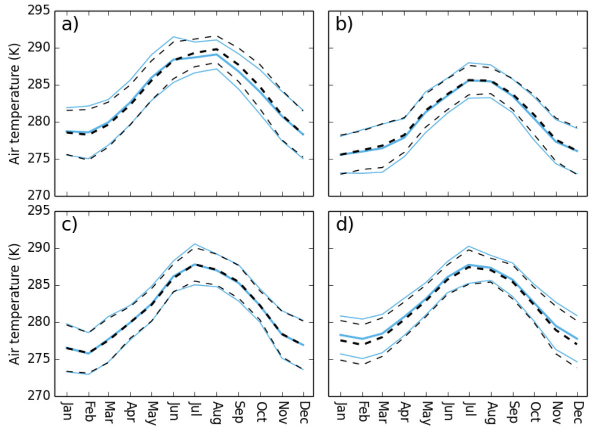

Figure 5. Mean monthly climatology of the dataset (blue, solid lines) and observed air temperatures (black, dashed lines), calculated for the period of observations. The thicker lines show the means, while the thinner lines show the standard errors on each measurement. Sites as in Fig. 4.

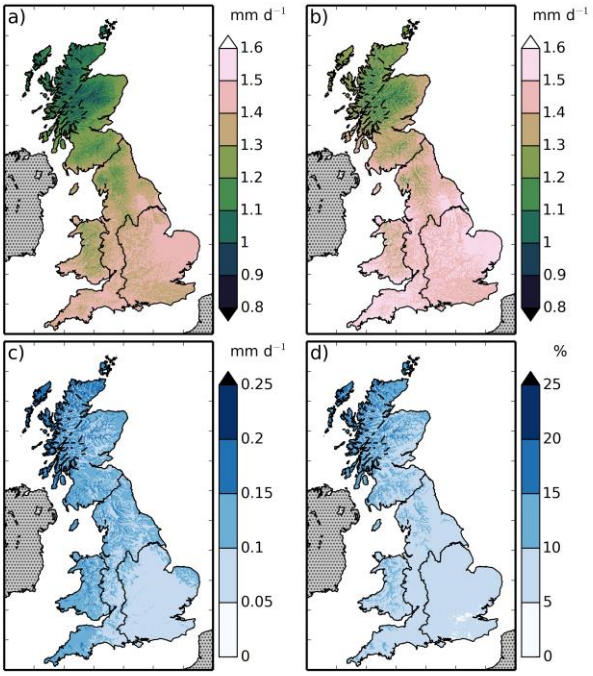

Figure 6. Mean a) PET, b) PETI, c) absolute difference between PETI and PET and d) relative difference calculated over the years 1961-2012.

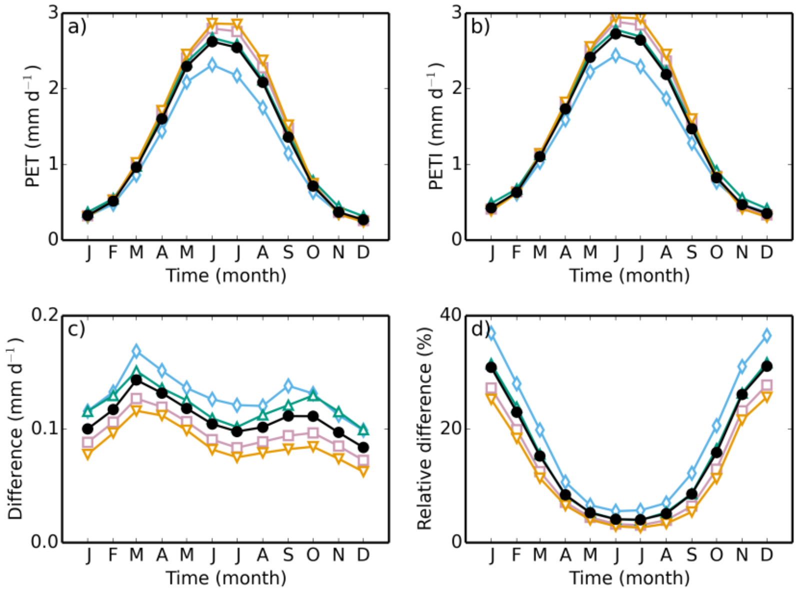

Figure 7. Mean monthly climatology of a) PET, b) PETI, c) absolute difference between PETI and PET, d) relative difference, for five different regions of Great Britain, calculated over the years 1961-2012. Symbols as in Fig. ~~2~~3.

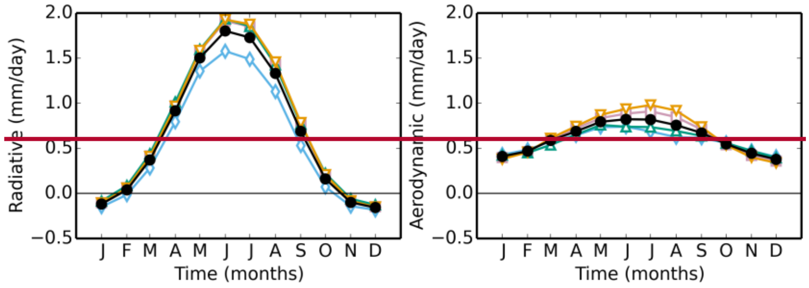

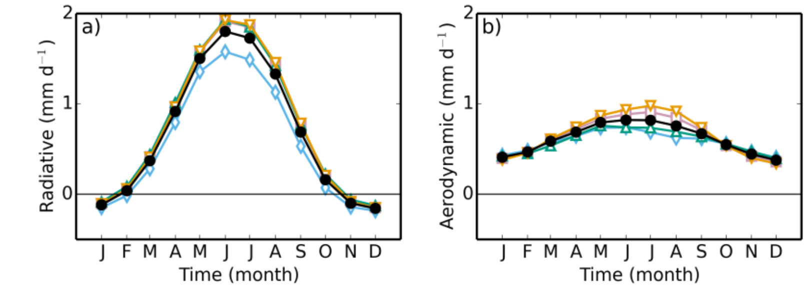

Figure ~~6~~8. Mean-monthly climatology of the a) radiative ~~(left)~~ and b) aerodynamic ~~(right)~~ components of the PET for five different regions of Great Britain, calculated over the years 1961-2012. Symbols as in Fig. ~~2~~3.

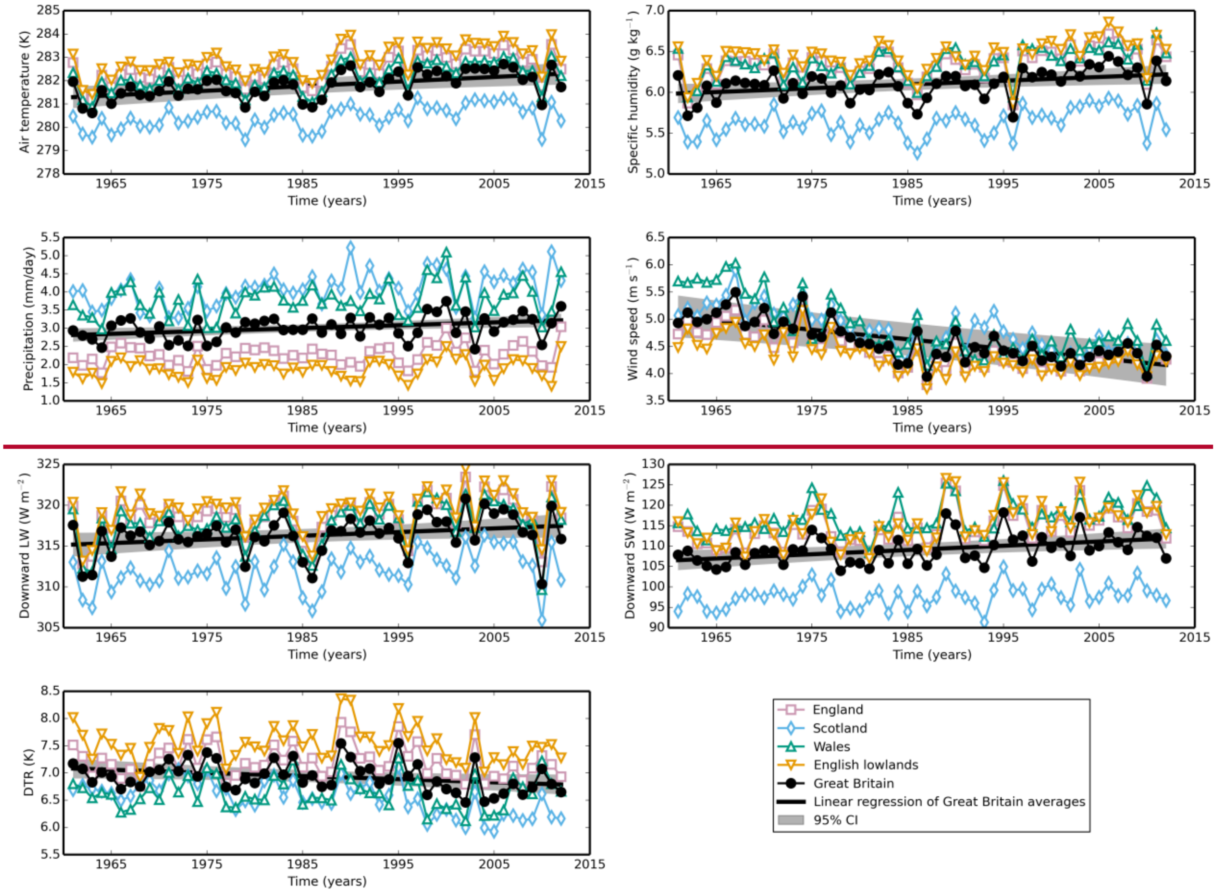
Air temperature (K)
Specific humidity (g kg^{-1})
Precipitation (mm/day)
Wind speed (m s^{-1})
Downward LW (W m^{-2})
Downward SW (W m^{-2})
DTR (K)
Time (years)
1965
1975
1985
1995
2005
2015
England
Scotland
Wales
English lowlands
Great Britain
Linear regression of Great Britain averages
95% CI

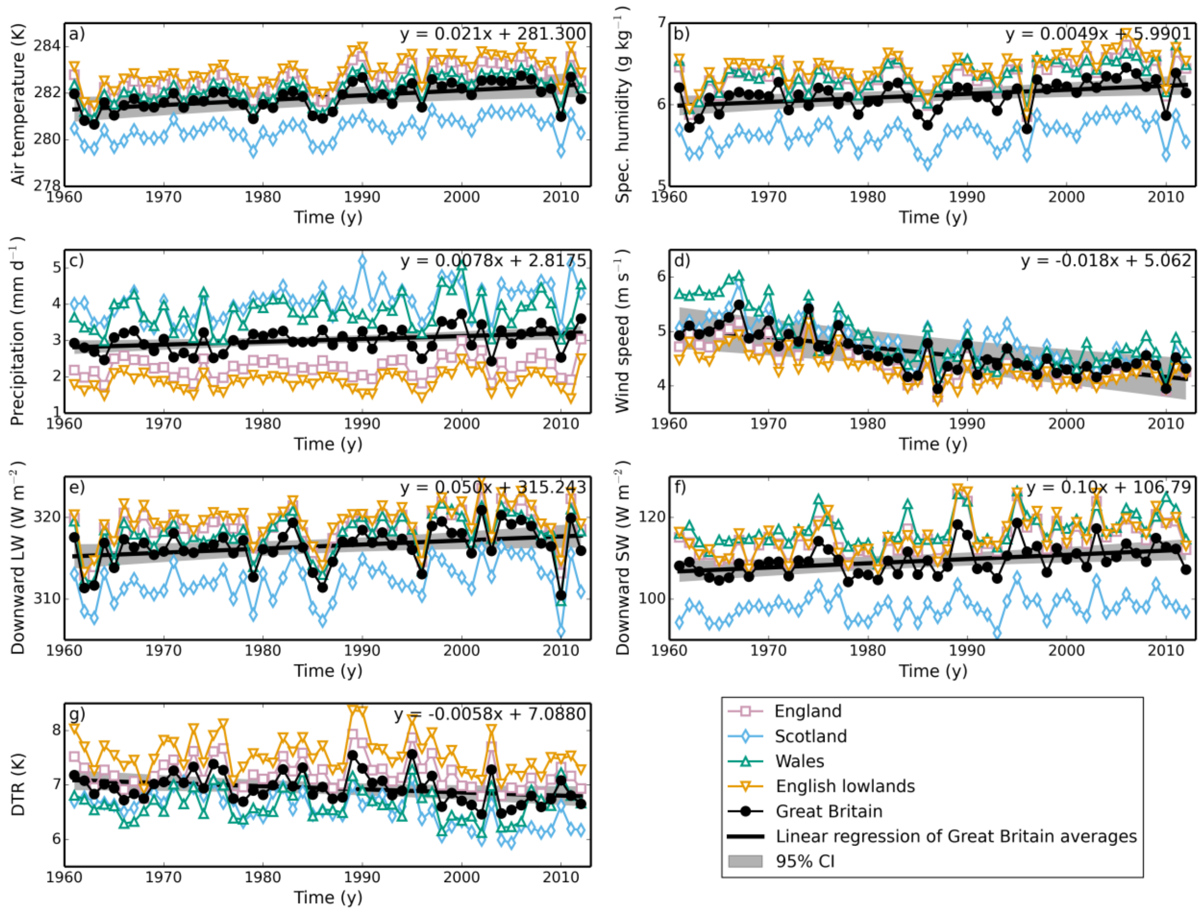

Figure ~~7~~9. Annual means of the meteorological variables, a) 1.2 m air temperature, b) 1.2 m specific humidity, c) precipitation, d) 10 m wind speed, e) downward LW radiation, f) downward SW radiation, g) daily air temperature range, over five regions of Great Britain. The solid black lines show the linear regression fit to the Great Britain annual means, while the grey strip shows the 95% ~~confidence interval~~CI of the same fit, assuming a non-zero lag-1 correlation coefficient. The equation of this fit is shown in the top right-hand corner of each plot.

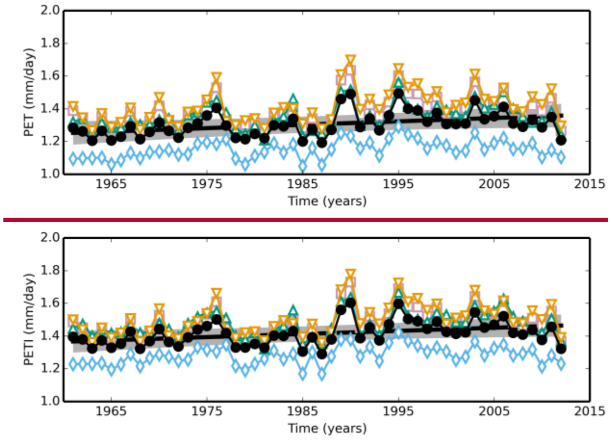

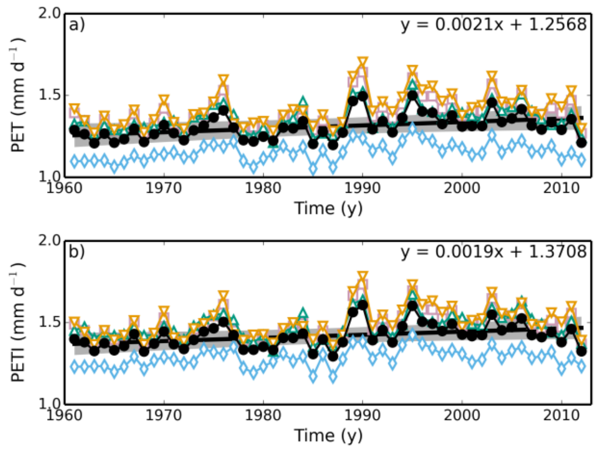

Figure ~~8~~10. Annual means of a) PET and b) PETI for five regions of Great Britain. Symbols as in Fig. ~~7.~~

9.

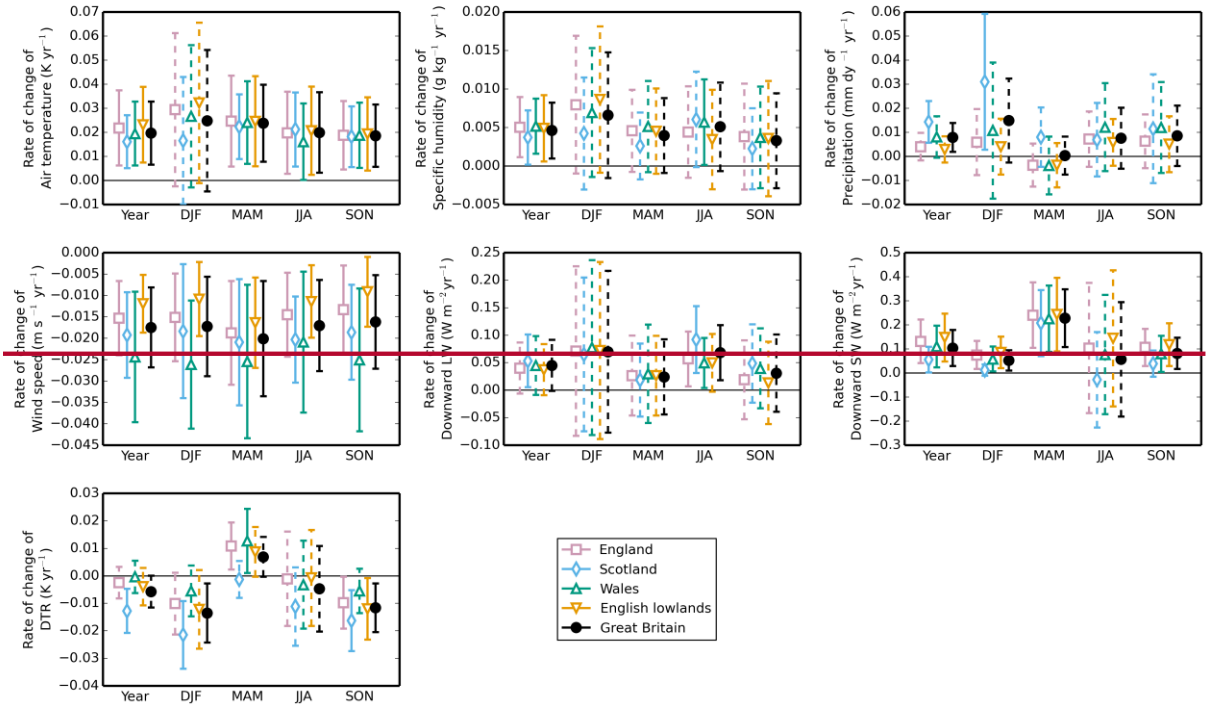
Rate of change of Air temperature (K yr^{-1})
Rate of change of Specific humidity (g kg^{-1} yr^{-1})
Rate of change of Precipitation (mm dy^{-1} yr^{-1})
Rate of change of Wind speed (m s^{-1} yr^{-1})
Rate of change of Downward LW (W m^{-2}yr^{-1})
Rate of change of Downward SW (W m^{-2}yr^{-1})
Rate of change of DTR (K yr^{-1})
Year
DJF
MAM
JJA
SON
England
Scotland
Wales
English lowlands
Great Britain

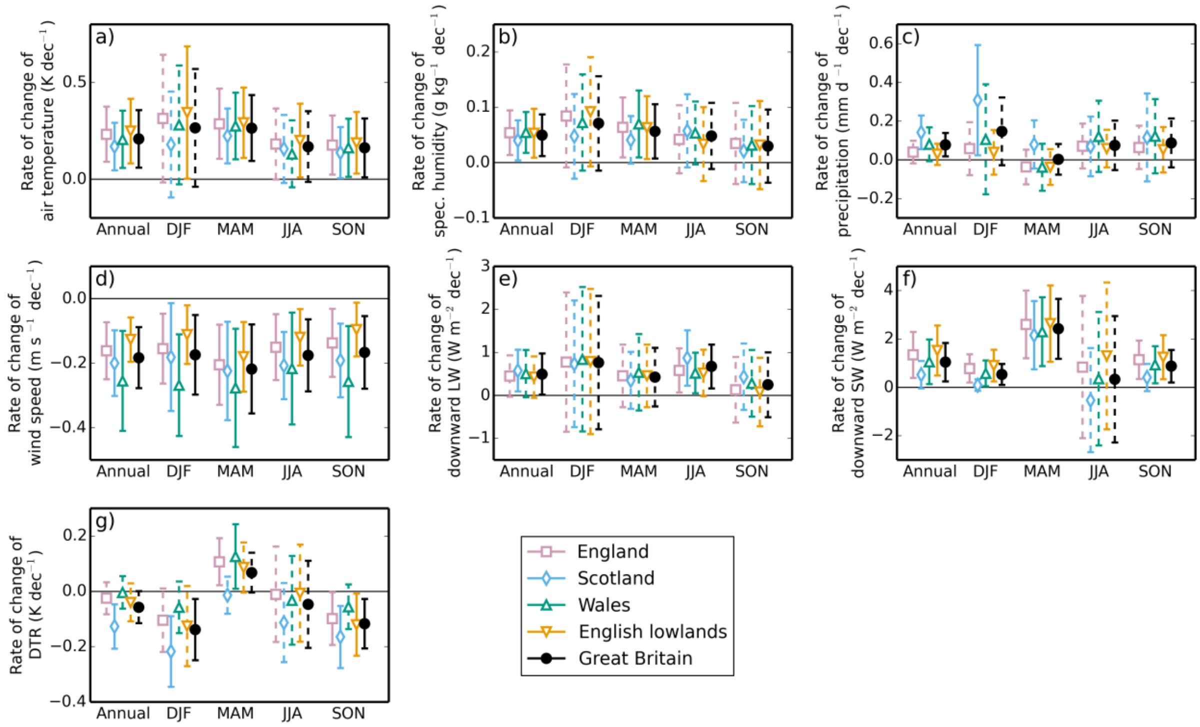

Figure 911. Rate of change of annual and seasonal means of meteorological variables, a) 1.2 m air temperature, b) 1.2 m specific humidity, c) precipitation, d) 10 m wind speed, e) downward LW radiation, f) downward SW radiation, g) daily air temperature range, for five regions of Great Britain. for the years 1961-2012. Error bars are the 95% confidence intervalsCI calculated assuming a non-zero lag-1 correlation coefficient. Solid error bars indicate slopes that are statistically significant at the 5% level, dashed error bars indicate slopes that are not significant at the 5% level.

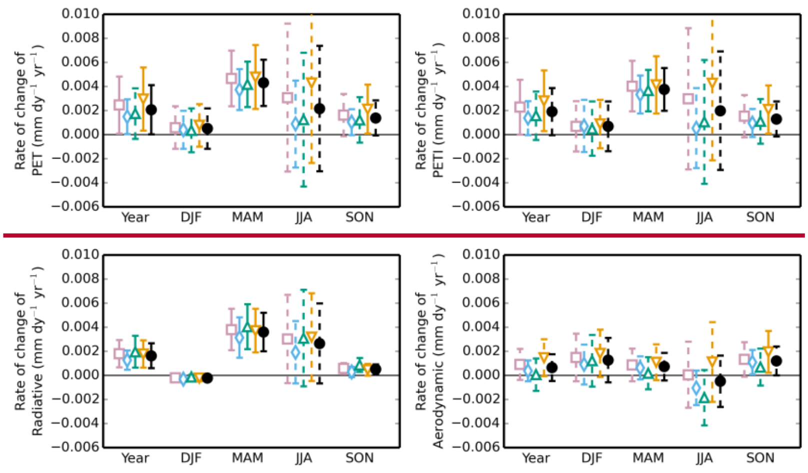
Rate of change of PET (mm dy⁻¹ yr⁻¹)
Rate of change of PETI (mm dy⁻¹ yr⁻¹)
Rate of change of Radiative (mm dy⁻¹ yr⁻¹)
Rate of change of Aerodynamic (mm dy⁻¹ yr⁻¹)
0.010
0.008
0.006
0.004
0.002
0.000
−0.002
−0.004
−0.006
Year
DJF
MAM
JJA
SON

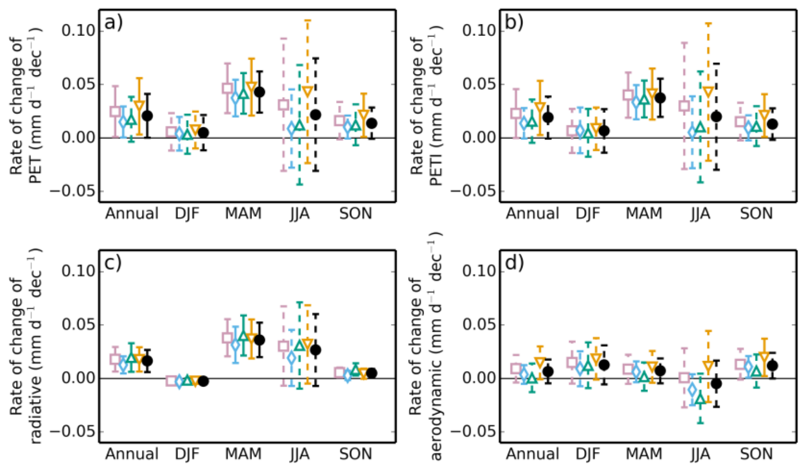

Figure ~~10~~12. Rate of change of annual and seasonal means of a) PET ~~(top left),~~, b) PETI ~~(top right),~~, c) the radiative component of PET ~~(lower left)~~ and d) the aerodynamic component of PET ~~(lower right)~~ for five regions of Great Britain~~.~~ for the years 1961-2012. Symbols as in Fig. ~~9~~11.

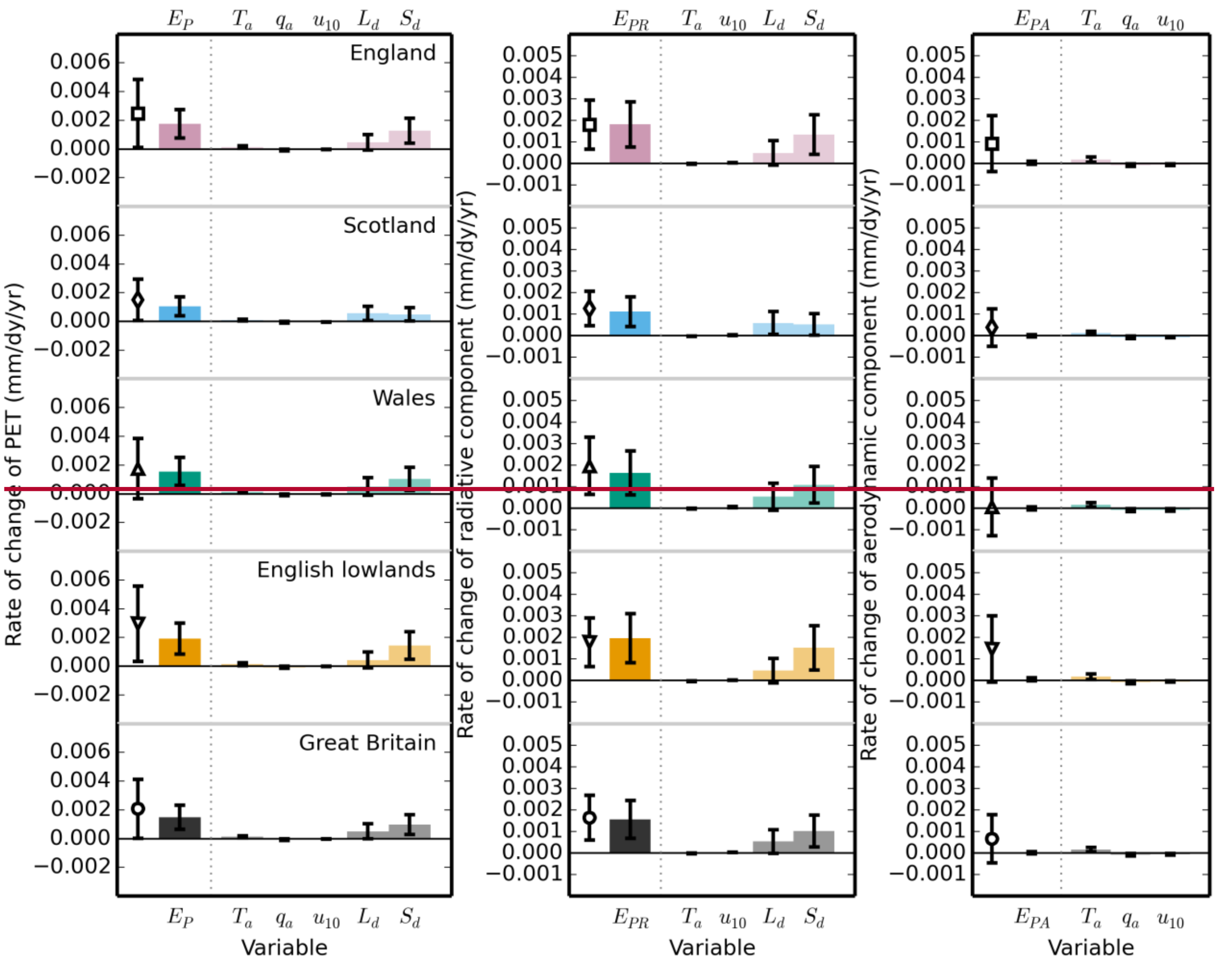
England
Scotland
Wales
English lowlands
Great Britain
Rate of change of PET (mm/dy/yr)
Rate of change of radiative component (mm/dy/yr)
Rate of change of aerodynamic component (mm/dy/yr)
E_P T_a q_a u_{10} L_d S_d
E_{PR} T_a u_{10} L_d S_d
E_{PA} T_a q_a u_{10}
Variable

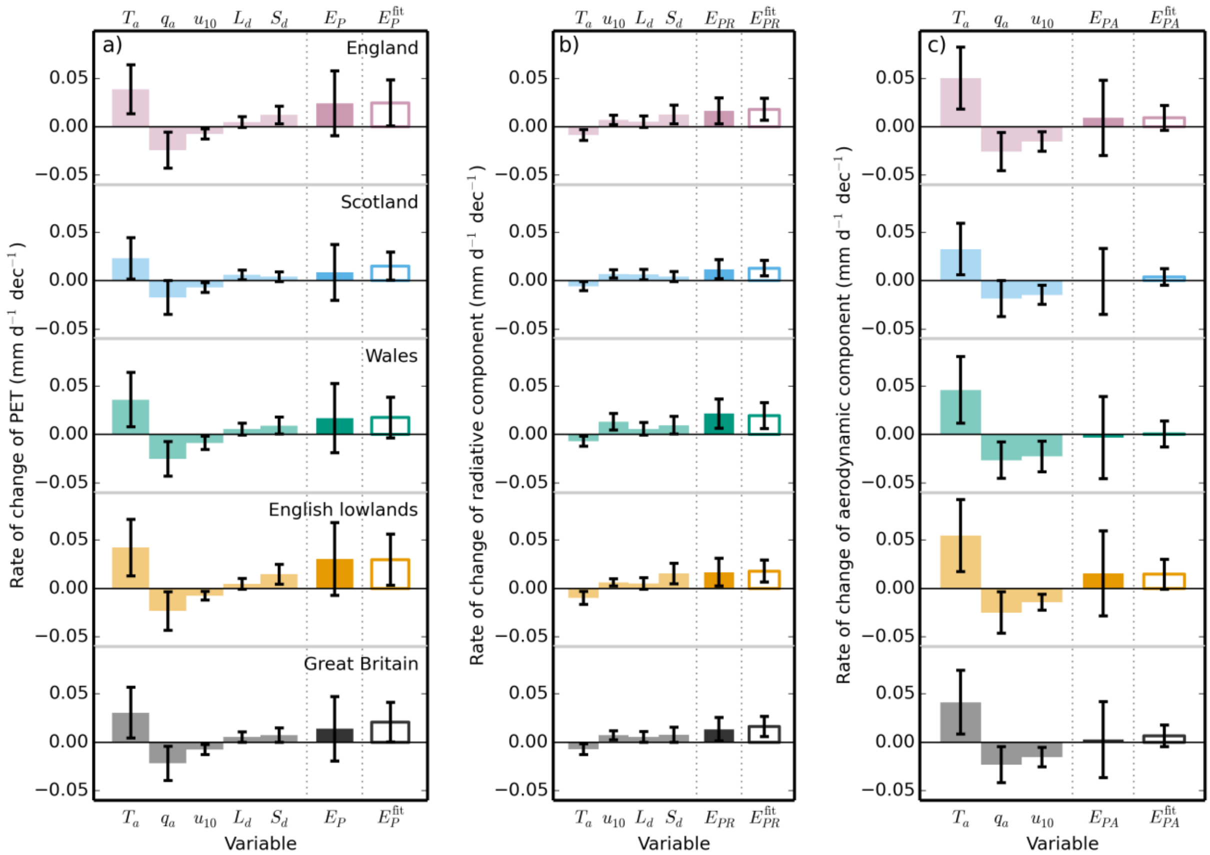

Figure ~~11~~13. The contribution of the rate of change of each meteorological variable to the rate of change of a) PET~~ (left),~~, b) the radiative component ~~(centre) ~~and c) the aerodynamic component~~ (right). In each panel~~. The first five (four; three) bars are the ~~left hand bar is~~contribution to the rate of change of annual mean PET ~~derived ~~from the rate of change of each of the variables~~. The rest of the columns show the contribution to that change from each of the variables. The ~~, calculated per pixel, than averaged over each region. Each bar has an error ~~bars show~~bar showing the 95% ~~confidence intervals~~CI on each value. ~~For~~Since the pixels are highly spatially correlated, we use the more conservative CI calculated by applying this analysis to the ~~left hand~~regional means. The next bar~~,~~ is the ~~symbols with error~~sum of the other bars ~~show~~and shows the attributed rate of change of annual mean PET. The final bar shows the slope and its associated ~~confidence interval~~CI obtained from the linear regression ~~(~~of the mean annual PET for each region.

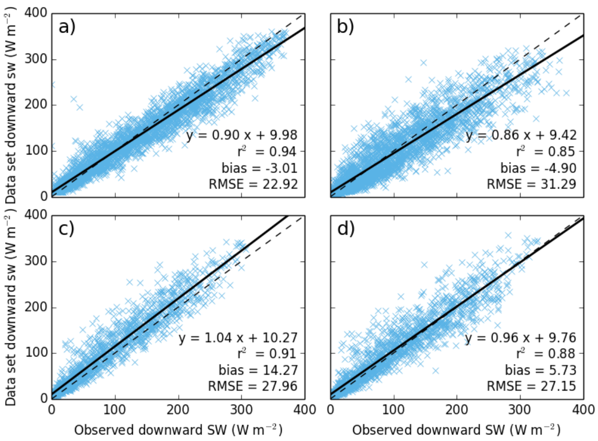

Figure A1. Plot of data set downward SW radiation against daily mean downward SW radiation at four flux sites. Symbols and sites as in Fig. ~~10).~~4.

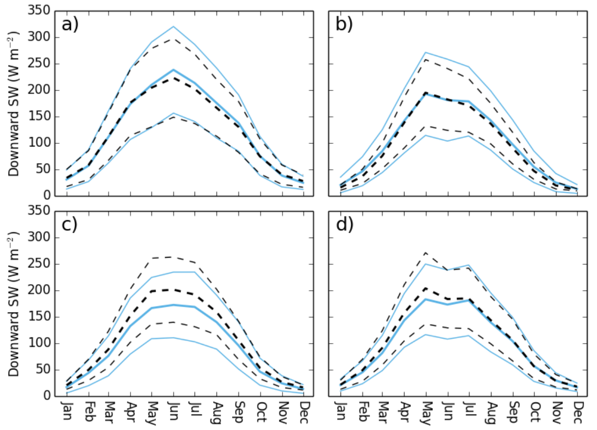

Figure A2. Mean monthly climatology of the dataset (blue, solid lines) and observed air temperatures (black, dashed lines), calculated for the period of observations. Symbols as in Fig. 5, sites as in Fig. 4.

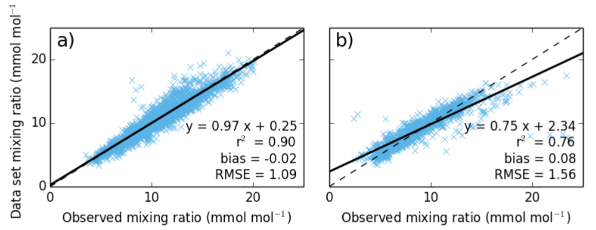

Figure A3. Plot of mixing ration calculated using dataset meteorology against daily mean observed mixing ratio at four sites. Symbols as in Fig. 4. The sites are a) Alice Holt and b) Griffin Forest.

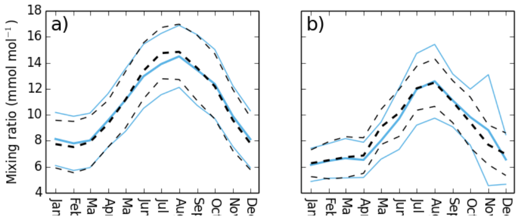

Figure A4. Mean monthly climatology of the dataset (blue, solid lines) and observed mixing ratio (black, dashed lines), calculated for the period of observations. Symbols as in Fig. 5. Sites as in Fig. A3.

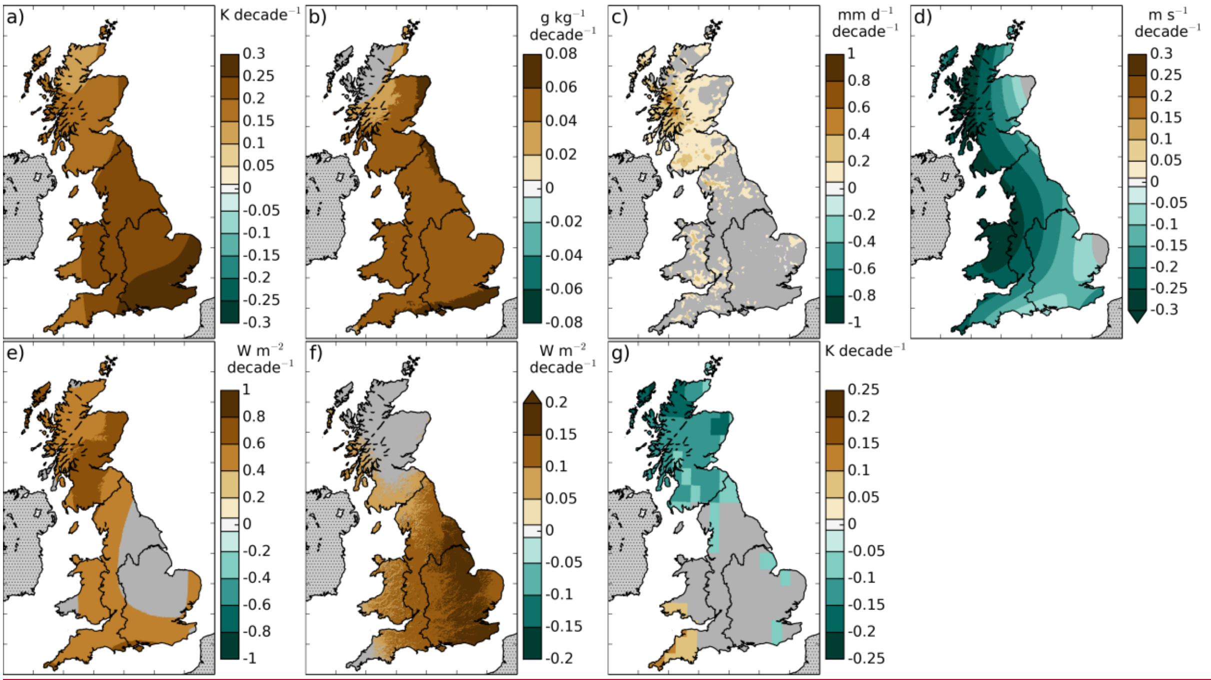

Figure B1. Rate of change of the meteorological variables, a) 1.2 m air temperature, b) 1.2 m specific humidity, c) precipitation, d) 10 m wind speed, e) downward LW radiation, f) downward SW radiation, g) surface air pressure, h) daily air temperature range over the period 1961-2012. Areas for which the trend was not significant are shown in grey.

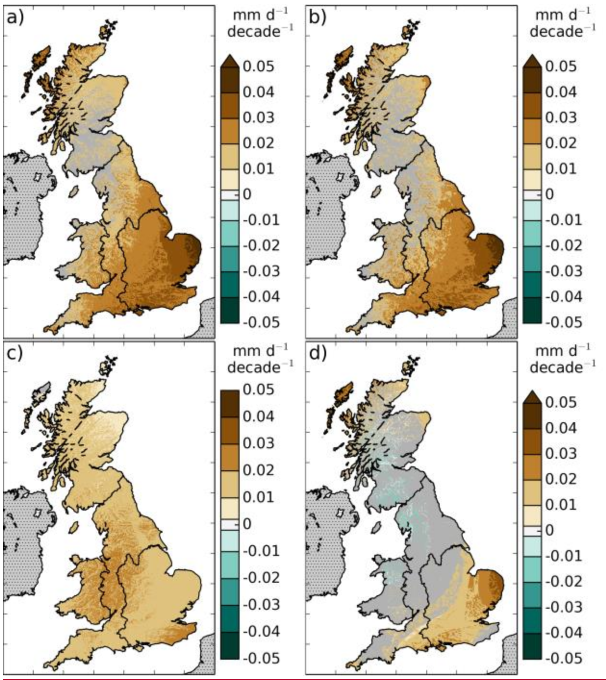

Figure B2. Rate of change of a) PET, b) PETI, c) the radiative component of PET, d) the aerodynamic component of PET over the period 1961-2012. Areas for which the trend was not significant are shown in grey.